EFFECT OF TRAFFIC LOADING ON MODAL PARAMETERS OF BRIDGES

by
Muhammet Furkan Çelenli
B.S., Civil Engineering, Bogazici University, 2008

Submitted to the Institute for Graduate Studies in
Science and Engineering in partial fulfillment of
the requirements for the degree of
Master of Science

Graduate Program in Civil Engineering
Boğaziçi University
2012

EFFECT OF TRAFFIC LOADING ON MODAL PARAMETERS OF BRIDGES

APPROVED BY:

Assist. Prof. Serdar Soyöz (Thesis Advisor)	. . . . .
Assoc. Prof. Hilmi Luş	. . . . .
Assist. Prof. ÇetinYılmaz	. . . . .

DATE OF APPROVAL: 27.08.2012

ACKNOWLEDGEMENTS

I would like to express my gratitude to all the people who in one way or another contributed to the development of this study. I would like to express my sincere appreciation to my advisor Assist. Prof. Serdar Soyöz; thank you for your valuable help in instructing, guiding and supporting me throughout the duration of this thesis.

Also, I would like to thank the members of my Master's thesis examination committee: Assoc. Prof. Hilmi Luş, and Assist. Prof. Çetin Yılmaz for their knowledgeable and in-depth comments and advice.

I am also grateful to Prof. Maria Feng and her research group, University of California, Irvine for providing the acceleration data from the Jamboree Road Overcrossing.

Finally, I would like to thank my family for their continuous support and encouragement.

ABSTRACT

EFFECT OF TRAFFIC LOADING ON MODAL PARAMETERS OF BRIDGES

This thesis primarily addresses the variation in identified modal parameters of bridges from traffic-induced vibration measurements. Effects of traffic loading on this variation are aimed to be analyzed. A typical mid-sized post-tensioned highway bridge, the Jamboree Road Overcrossing (JRO) that is located in Irvine, CA, US was used as a case study. The JRO was monitored over a five-year period and 1707 traffic-induced vibration data sets were collected through 13 acceleration sensors. First of all, modal parameters and structural properties are identified by using the Frequency Domain Decomposition (FDD) method and radial basis neural networks, respectively. Variations up to 10% in modal frequencies and 6% in structural properties are observed under the same environmental conditions over the same period. Then, in order to investigate the reasons of the variations, three different finite element analyses are carried out. While static mass and moving load analyses are conducted by the initial finite element model of the JRO, correlated white noise analysis is conducted by a single span finite element beam model. As a conclusion, it is observed from the results of static mass analysis that additional masses have significant contributions in modal mass of the system. Increase in the modal mass, then, results in decrease in natural frequencies. Numbers, locations and quantities of the additional masses are the determinative factors of this decrease. Furthermore, responses of the moving load and correlated white noise analyses are obtained. Afterwards, modal parameters of the models are identified from these responses by using FDD method. As a result, speed of the moving load causes significant variations in the identified natural frequencies. It is also concluded that correlated white noise results in suppressed modes, pseudo peaks and shifts in the identified natural frequencies.

ÖZET

TRAFİK YÜKÜNÜN KÖPRÜLERİN MODAL PARAMETRELERİ ÜZERİNDEKİ ETKİSİ

Bu tez, öncelikle trafik kaynaklı titreşim ölçümlerinden belirlenmiş olan köprülerin modal parametrelerindeki değişkenliğe değinmektedir. Trafik yükünün, bu değişkenlik üzerindeki etkilerinin analiz edilmesi amaçlanmıştır. Tipik bir orta ölçekli, ardgermeli otoyol köprüsü olan, Irvine, CA, ABD de bulunan, Jamboree Yolu Üstgeçidi (JYÜ) bir durum çalışması olarak kullanılmıştır. JYÜ beş yıllık bir dönem boyunca izlenmiş ve 1707 trafik kaynaklı titreşim veri setleri, 13 ivme sensörü aracılığıyla toplanmıştır. Öncelikle, modal parametreler ve yapısal özellikler sırasıyla, Frekans Ortamında Ayrıştırma (FOA) yöntemi ve radyal tabanlı sinir ağları kullanılarak belirlenmiştir. Aynı çevre koşulları altında ve aynı dönem boyunca, modal frekanslarda %10'a ve yapısal özelliklerde %6'ya kadar değişkenlikler gözlemlenmiştir. Daha sonra, değişkenliklerin nedenlerini incelemek amacıyla, üç farklı sonlu elemanlar analizi yapılmıştır. Statik kütle ve hareketli yük analizleri YJÜ'nün ilk sonlu elemanlar modeli ile yapılırken, ilişkili beyaz gürültü analizi ise tek açıklıklı bir kirişin sonlu elemanlar modeli ile yapılmıştır. Sonuç olarak, statik kütle analizi sonuçlarından, ek kütlelerin, sistemin modal kütlesine önemli katkılarının olduğu gözlemlenmiştir. Modal kütledeki artış, daha sonra, doğal frekanslarda azalma ile sonuçlanır. Ek kütlelerin sayısı, konumu ve miktarı, bu azalmayı belirleyen faktörlerdir. Buna ek olarak, hareketli yük ve ilişkili beyaz gürültü analizlerinin tepkileri elde edilmiştir. Daha sonra, bu tepkilerden, modellerin modal parametreleri FOA yöntemi kullanılarak belirlenmiştir. Sonuç olarak, hareket eden yükün hızı, tanımlanan doğal frekanslardaki değişkenliklerde önemli farklılıklara sebep olmuştur. İlişkili beyaz gürültünün, bastırılmış modlar, aldatıcı pikler ve belirlenen doğal frekanslardaki kaymalar ile neticelendiği, ayrıca sonuçlandırılmıştır.

TABLE OF CONTENTS

ACKNOWLEDGEMENTS iii
ABSTRACT iv
ÖZET v
LIST OF FIGURES viii
LIST OF TABLES xii
LIST OF SYMBOLS xiii
LIST OF ACRONYMS / ABBREVIATIONS xiv
1. INTRODUCTION 1
1.1. General 1
1.2. Motivation of Structural Health Monitoring 2
1.3. Literature Review 3
1.4. Statement of the Problem and Objectives 12
1.5. Scope and Outline 13
2. STRUCTURAL IDENTIFICAION 14
2.1. System Identification 14
2.2. Output-Only Structural System Identification Methods 17
2.2.1. Frequency Domain Decomposition 18
2.3. Jamboree Road Overcrossing 20
2.3.1. Instrumentation of the JRO 21
2.3.2. Acceleration Data of the JRO 23
2.3.3. Identified Modal Parameters of the JRO 25
2.4. Variation in Identified Modal Parameters 29
2.4.1. Discussion in Identification of the Data in Segments. 31
3. FINITE ELEMENT MODEL AND STRUCTURAL PROPERTIES 33
3.1. General 33
3.2. Bridge Properties 33
3.3. Boundary Conditions and Soil Springs 36
3.4. Modal Analysis Results. 37
3.5. Identification of Structural Properties 39

4. EFFECT OF TRAFFIC LOADING 44
4.1. General 44
4.2. Static Mass Analyses 44
4.3. Moving Load Analysis of a Single Span Beam 47
4.3.1. Analytical Solution of Moving Load Problem 47
4.3.2. Correlated White Noise Analysis of a Single Span Beam 50
4.4. FEM Analysis of Moving Load Problem of the JRO 54
4.5. Discussion in Cross-Correlation and Speed 61
5. CONCLUSIONS AND RECOMMENDATIONS 64
5.1. Conclusions 64
5.2. Recommendations 64
REFERENCES 66

LIST OF FIGURES

Figure 2.1. Visualization of a dynamic system. 15

Figure 2.2. The satellite view of the JRO. 20

Figure 2.3. Plan and side views of the JRO. 21

Figure 2.4. The layout of the sensors. 22

Figure 2.5. Wireless antenna and solar panels. 23

Figure 2.6. Typical acceleration responses of the channel (a) 6 (b) 4 (c) 15 (d) 14 (e) 13. 24

Figure 2.7. Acceleration response of channel 6 on 31st of May, 2002. 25

Figure 2.8. First singular values of the PSD matrice and peaks. 26

Figure 2.9. First and second singular values of the PSD matrice. 26

Figure 2.10. Identified mode shapes of the JRO corresponding to the (a) first (b) second (c) third (d) fourth mode. 27

Figure 2.11. First four identified modal frequencies of the JRO. 28

Figure 2.12. Identified modal frequencies of the (a) first (b) second (c) third (d) fourth mode. 29

Figure 2.13. Changes between the first modal frequencies identified from consecutive data sets. 30

Figure 2.14. Identification of an acceleration data with different segments. 31

Figure 2.15. First modal frequencies identified from different segment. 31

Figure 3.1. Technical drawings of box section girder and columns. 34

Figure 3.2. Plan view of the JRO from technical drawing.. 34

Figure 3.3. Box section girder element and properties. 35

Figure 3.4. Soil spring calculations according to FHWA. 36

Figure 3.5. Constraints of the FEM of the JRO.. 37

Figure 3.6. 3D view of the constructed FEM of the JRO with existing constraints. . 37

Figure 3.7. Mode shapes of the FEM of the JRO: (a) first (b) second (c) third (d) fourth (e) fifth mode.. 38

Figure 3.8. Extraction of structural properties by using NN. 41

Figure 3.9. A two-layer radial basis NN. 41

Figure 3.10. Identified coefficients for (a) superstructure mass (b) column mass (c) superstructure stiffness (d) column stiffness (e) soil spring at A1 (f) soil spring at A4.. 42

Figure 4.1. Node numbers for the static mass analysis. 45

Figure 4.2. A moving load model. 47

Figure 4.3. FEM for correlated white noise analysis. 50

Figure 4.4. White noise input. 51

Figure 4.5. PSD of the white noise input.. . . . 51

Figure 4.6. A typical acceleration output of the node 4. 52

Figure 4.7. Singular values of PSD matrices for (a) Case 1 (b) Case 2 (c) Case 3 (d) Case 4 (e) Case 5. 53

Figure 4.8. FEM of the moving load.. . . . 54

Figure 4.9. Singular values of PSD matrices for Type 1 analyses. 55

Figure 4.10. Singular values of PSD matrices for Type 2 analyses. 56

Figure 4.11. Singular values of PSD matrices for Type 3 analyses. 56

Figure 4.12. Singular values of PSD matrices for Type 4 analyses. 57

Figure 4.13. Singular values of PSD matrices for Type 5 analyses. 57

Figure 4.14. Identified first modal frequencies from moving load analyses for (a) Type 1 (b) Type 2 (c) Type 3 (d) Type 4 (e) Type 5. 58

Figure 4.15. Singular values of PSD matrice for Type 4 analysis with 150 km/h speed. 59

Figure 4.16. Singular values of PSD matrice for Type 3 analysis with 30 km/h speed. 59

Figure 4.17. Singular values of PSD matrice for Type 2 analysis with 60 km/h speed. 60

Figure 4.18. Singular values of PSD matrice for Type 3 analysis with 90 km/h speed. 60

Figure 4.19. Singular values of PSD matrice for Type 5 analysis with 75 km/h speed. 60

Figure 4.20. Effect of the speed on dynamic amplification factor.. 61

Figure 4.21. Well separated acceleration peaks for time delay calculation. 62

Figure 4.22. Disturbances of the different vehicles. 63

LIST OF TABLES

Table 2.1. Identified modal frequencies of the JRO by different authors. 28

Table 3.1. Structural Properties of the FEM of the JRO.. 37

Table 3.2. Modal frequencies of the FEM of the JRO.. 39

Table 3.3. An example input-output set of FEM analyses of the JRO. 40

Table 3.4. Structural property constants. 40

Table 4.1. Changes in the modal frequencies of the single lumped mass analysis.. . 46

Table 4.2. Changes in the modal frequencies of the double lumped mass analysis. . 47

Table 4.3. Properties of the structural elements and boundary conditions of FEM. . 51

Table 4.4. Case analyses and results.. 52

LIST OF SYMBOLS

c	Constant speed of the point load
E	Modulus of elasticity
g	Gravitational acceleration
$H(\omega)$	Frequency response function matrix
Hz	Hertz
I	Moment of inertia
j	Mode number
k	An arbitrary constant
l	Length of the beam
m	Unit mass of the beam
N	Newton
P	Point load
s	Second
$S_{XX}(\omega)$	Power spectral density of input $X(t)$
$S_{YY}(\omega)$	Power dpectral density of response $Y(t)$
t	Time
$U(\omega)$	Unitary matrix containing the singular vectors
$v(x,t)$	Deflection of the beam
$V(j,t)$	Integral transform of $v(x,t)$
x	Length variable of the beam
$X(t)$	Input
$Y(t)$	Output
$\Lambda(\omega)$	Diagonal matrix containing the transfer functions
$\sum(\omega)$	Diagonal matrix containing the singular values
Φ	Unitary mode shape matrix
ω	Circular frequency
ω_b	Circular frequency of damping

LIST OF ACRONYMS / ABBREVIATIONS

AASHTO	American association of state highway and transportation officials
ARMA	Autoregressive moving-average method
CA	California
3D	Three dimensional
ERA	Eigensystem realization algorithm
FE	Finite element
FEM	Finite element model
FDD	Frequency domain decomposition
FHWA	Federal highway administration
FRF	Frequency response function
FROO	Fairview road on-ramp overcrossing
JRO	Jamboree road overcrossing
ITD	Ibrahim time domain
N/A	Not applicable
NBIS	National bridge inspection standards
NN	Neural network
PSD	Power spectral density
RC	Reinforced concrete
SHM	Structural health monitoring
SI&A	Structure inventory and appraisal
SISO	Single-input single-output
SVD	Singular value decomposition
UCI	University of California, Irvine
US	United States
VBI	Vehicle-bridge interaction
WSO	West street on-ramp

1. INTRODUCTION

1.1. General

Determining static and dynamic properties of structures is the main objective in structural engineering. Static characteristics basically depend on load bearing capacities of structural elements such as axial, buckling, bending, torsion and shear load capacities. Static properties have direct effects on dynamic characteristics generally named as ‘modal parameters’: modal frequency, modal damping ratio and corresponding mode shapes.

Structural properties are expected to satisfy the design limits over the structure’s lifetime. Initial condition of a structure can be defined as the undamaged state. This condition is supposed to be very close to the design properties; however, a structure cannot maintain its initial properties over its lifetime. Aging, fatigue, degradation, corrosion, earthquakes are some of the many reasons for this situation. All these effects are considered in design steps and structures are always designed with a factor of safety to be on the safe side within the design limits.

In addition, there may be unexpected problems: rapid changes in material or sectional properties, changes in climate, changes in service loads, changes in the sequence and characteristics of earthquakes, etc. These expected and unexpected reasons lead to unfavorable changes in structural properties and may even cause damage.

Farrar *et al*. [1] describe the damage as the changes between the two stages of the system that affect its current and future performance. His study mentions that damage begins at material level. Changes in the boundary conditions and system connectivity are also considered within the description of damage. Aging of concrete is a widely known issue in civil engineering. Load bearing capacity of concrete decreases over time. This aging causes a decrease in elastic modulus of concrete and that leads to a decrease in bending capacity. Then, decrease in bending capacity directly causes a decrease in dynamic stiffness of the structure.

Due to these reasons, it is well known that there is always a change in structural properties, but how fast and how severe this change would be the most important point in this concept. Another important issue is whether this change is normal or abnormal. In other words, is there any damage or not? Assessment for the remaining lifetime of the structure after the change is the final concern. To answer these questions, first of all we have to be able to identify the current condition of the structure. Secondly, we have to compare our current condition with the previous known conditions or initial design parameters.

1.2. Motivation of Structural Health Monitoring

Structural Health Monitoring (SHM) can be described as the process of assessment of different conditions including the current one and estimates for the future conditions of structure by identifying the properties of the structure frequently (at least two different times).

The information of changes in structural properties and severity of these changes make it possible to make reliable decisions on the conditions of these structures. Making reliable decisions is very crucial especially for life safety aspects and then economical aspects such as investment in bridges for maintenance or reconstruction. These aspects make SHM very important for the community. The fundamental objectives of SHM in Civil Engineering are listed as follows:

- Identifying the current state of structures
- Identifying the damage
- Making decisions on modification of existing structures
- Making estimations on future performance of structures
- Improving the knowledge for future designs

1.3. Literature Review

A systematic inspection and reporting system about conditions of bridges is very important for safety and investment for bridges. This system should be in accordance with the National Bridge Inspection Standards (NBIS) [2]. The Federal Highway Administration (FHWA) Recording and Coding Guide for the Structure Inventory and Appraisal (SI&A) of the Nation's Bridges (Coding Guide) [3] is the main guide for inspection systems. The designated inspection frequency and qualification, which are regulated by the NBIS, are included in the Coding Guide. The Coding Guide includes definitions of basic terms, data items that have to be included in inspections, SI&A sample sheets, rating methods and examples of four main ratings, which are:

- Condition rating
- Capacity rating (Operating and Inventory Rating)
- Appraisal rating
- Sufficiency rating

Structural elements of bridges such as deck, superstructure, substructure, channels and culverts are the main items for the condition ratings. The conditions of the structural elements are the main indicators of structural health. The accuracy and reliability of visual inspection is very crucial to make true decisions.

On the other hand, there are some drawbacks of visual inspection. Phares *et al*. [4] stated that the limitations of visual inspection have a direct influence on its reliability. Results from his study related with the accuracy and reliability of routine inspection documentation were summarized. Forty nine inspectors from 24 states attended for inspection of seven different bridges according to the Coding Guide. Their ratings about the structural elements, hand notes and photos taken by them are compared. It was shown that there is a significant variability between inspection documentations, mostly in ratings of structural conditions and also handwritten inspection notes and photos for critical locations. The main reason for this variability is the qualitatively described rating methods in the Coding Guide.

In 2008, The Long-Term Bridge Performance Program [5] was initiated by FHWA for a 20-year period. The main objective of this program is collecting reliable and quantitative information from bridges to establish an extensive database. Vibration based continuous monitoring of bridges under service and earthquake loads are being explored.

With the increasing significance of the quantitative assessment for inspections, numerous studies have been performed to develop reliable and accurate system identification methodologies for structures.

Safak [6] carried out a study that includes the discrete-time representation of Single-Input Single-Output (SISO) systems, models for SISO systems with noise, the concept of stochastic approximation and the recursive prediction error method for system identification and adaptive control. In the first part, a brief review on the theory of stochastic-adaptive modeling, identification and control of dynamic systems based on discrete-time domain was given. In the second part, five different examples were presented for adaptive methods which are mentioned in the first part. Advantages of adaptive methods were listed as follows:

- removing the noise from the signal over the whole frequency band
- tracking time-varying characteristics of systems
- opportunity for controlling unknown systems

The importance of selection of the model type, model order and initial values was also mentioned to get accurate identification results and guidelines for these aspects were discussed.

A discrete-time domain system identification technique using discrete-time linear filters was represented by Safak [7] in another study. In practice, a real-world structure was identified by using this technique. It was shown that proposed technique is valid for linear structures. In contrast to linear structures with wide-band measurement noise, for the case of nonlinear structures or existence of noise including dominant frequencies, adaptive identification methods are suggested instead of proposed technique.

Many structural system identification techniques were reviewed by Ghanem and Shinozuka [8, 9]. Maximum likelihood, extended Kalman filter, recursive least squares (with/without windows) and recursive instrumental variable (with/without filter) techniques were studied. Two different laboratory structures, which were subjected to earthquake simulations, were identified by using these techniques. The importance of robustness, simplicity and reliability for system identification techniques and the importance of the measurement locations were pointed out.

Another study on system identification for linear structures subjected to earthquake excitation was conducted by Lus *et al*. [10]. This study proposed a system identification technique based on eigensystem realization algorithm and observer/Kalman filter identification approach for identification process of structural elements. Efficiency of proposed methodology was demonstrated by applying this methodology on a numerical model and a real-world structure. Effects of noise and inadequate instrumentation were also pointed out and identified results were excellently converged to real structural properties.

Up until now, numerous studies have been completed and so many identification techniques were developed. Each technique involves different assumptions and different methodologies. Many of them are related to special cases or special structures. Many reviews about structural identification techniques and SHM were reported. These reviews generally include the state-of-the-art of the SHM and categorize the system identification methods into groups.

Doebling *et al*. [11] reported an extensive review of hundreds of technical literature related to structural damage identification methodologies based on structural vibration measurements. This report contains developments of these methodologies and applications. Structural identification applications of so many types of structures including beams, trusses, plates, shells, frames, aerospace structures, bridges and other large engineering structures like offshore platforms are also categorized into groups. At the end the critical issues for future studies were summarized.

An updated version of the report, presented by Doebling *et al*. [11] was published by Sohn *et al*. [12]. This new report organized technical literature related to four basic steps of a statistical pattern recognition paradigm: (I) operational evaluation, (II) data acquisition, fusion, and cleansing, (III) feature extraction and information condensation, and (IV) statistical model development for feature discrimination. Reviewed literatures are then categorized by application types again. Projects, web sites, conferences and technical journals related to SHM are also given in another chapter. Finally current condition of SHM technologies and recommended research areas were summarized.

Maia and Silva [13] conducted a study considering a general view of modal identification techniques including a historical summary, various types of classification groups and brief information of some modal identification techniques. Three main classification groups were represented based on identification domain, number of input-output locations and the way of identification for structural properties. The first classification group consists of frequency and time domain identification techniques. The second group classification types of techniques are given as follows:

- Single-Input Single-Output
- Single-Input Multiple-Output
- Multiple-Input Multiple-Output
- Multiple Input Single-Output

The third classification group consists of direct and indirect identification methods. Direct identification methods result in structural properties in terms of stiffnesses, masses and damping coefficients. However, indirect identification methods result in modal parameters which are modal frequencies, corresponding mode shapes and modal damping ratios.

A review on SHM of civil infrastructure was completed by Brownjohn [14]. This review consists of the motivation, recent history and fundamental objectives of SHM applications of civil infrastructure. Case studies on typical structures such as dams,

bridges, offshore platforms, nuclear plants, tunnels, excavations, buildings and towers were also presented. Lastly it mentions recent SHM technology, problems and limitations.

Carden *et al*. [15] presented the current state of vibration based condition monitoring of structures. Numerous types of algorithms based on time, frequency and modal domains were reviewed. It was mentioned that real-world structures are subjected to environmental effects and no algorithm is present that reliably filters these effects. The importance of the number of data locations was remarked that more sensors or data locations provide a greater success in damage detection. The main conclusion was that there was not a universal algorithm that can identify any types of structure reliably and any algorithm for prediction of the remaining service life of the structures is present.

As mentioned above, many different system identification methodologies were developed for many different structural applications. Some of the important studies on structural identification of bridges are summarized.

Choi *et al*. [16] conducted a study about change in ratings of structural properties quantitatively over a period by using system identification techniques. A frequency domain identification technique was used for extraction of physical properties of a concrete box girder bridge. Modal parameters were identified by frequency response functions. Along the study four measured data sets were collected. Between the third and fourth data set, an earthquake was occurred and stiffness change due to the earthquake was quantitatively determined. A finite element model of the bridge was constructed, results from real case structure and numerical model were compared and identification process was validated.

An experimental study on damage assessment of jacketed reinforced concrete columns was conducted by Feng and Bohng [17]. Two half-scale jacketed RC columns were analyzed under cyclic loadings to reach several damage levels. Before and after all cyclic loadings, vibration tests are conducted for each column. Changes in stiffness of the columns were extracted quantitatively based on identified modal parameters of the columns after vibration tests by using neural network algorithm. Although there was no

visible damage in columns, change in stiffness was obtained related to changes in modal frequency and damping ratio for each column after cycling loadings.

Guan *et al*. [18] implemented a web-based health monitoring system using wireless technology in their study. A fiber reinforced polymer composite bridge was instrumented with accelerometers, strain gauges, temperature sensors and a video camera to perform a long-term performance monitoring. An automated real time system identification algorithm was used for the identification of changes in structural properties. In addition, a strong wireless communication system was established for the data transmission from the test field to the servers and rapid access was ensured for authorized persons to check the current health status of the bridge through a web-based interface.

Feng *et al*. [19] carried out a study about using the results of ambient vibration measurements with limited data locations to estimate structural properties of a finite element model of a large scale structure. Modal parameters were estimated from measured data by appropriate system identification techniques including random decrement method. An initial finite element model was constructed using design drawings and it was updated with the findings from the field tests.

Feng *et al*. [20] conducted another study to construct and update a baseline finite element model of a bridge by neural network based system identification technique. To demonstrate this baseline methodology, two highway bridges were instrumented and vibration data from these structures were used. Modal parameters of these two bridges were estimated by using the frequency domain decomposition, random decrement and peak picking methods, separately. It was pointed out that mode shapes estimated by frequency domain decomposition method appear more reliable than peak picking method. Initial finite element models were constructed and 5000 different variations of these initial models were created by changing their eighth different structural property constants. 5000 different models result in 5000 different modal parameters. A back propagation Neural Network (NN) was used for mapping of these 5000 set of input and output. This NN gives the structural properties of the bridges related to the identified modal parameters so it

becomes very easy to determine actual structural properties at any particular time, in long-term monitoring periods.

An extensive report of a comprehensive study on long-term structural performance monitoring of bridges was published by Feng *et al*. [21]. This is the second report from this study. In the first report [22] instrumentation of two newly constructed bridges (Jamboree Road Overcrossing (JRO) and West Street On-Ramp (WSO)), preliminary measurements and vibration data analyses were demonstrated. In this current report a new bridge (Fairview Road On-Ramp Overcrossing (FROO)) was added to the project. Besides the vibration and strain data analyses, static load, dynamic load, breaking and bumping tests were conducted through this project. The main objective was the development of new methodologies for analyzing the measured data and estimating the on-going condition of the structure. While a Bayesian updating method and a neural network method were developed for identification of superstructure parameters from traffic-induced vibration measurements, an extended Kalman filter method and a neural network method were formulated for identification of structural properties of columns under lateral excitations. In addition, a unique traffic excitation model was proposed instead of white noise assumption. This model was developed by using vision-based traffic monitoring information to make identified parameters more reliable. Developed methods were verified with seismic shaking table tests of a reinforced concrete bridge model. Effectiveness of proposed methods was demonstrated. Finally, identified modal parameters from long-term monitoring data were developed into a database. By using this database, structural stiffnesses were extracted and compared by results from different system identification methodologies developed previously. Compared results were consistent with each other. As a result of developing the database, a variation in the identified natural frequencies and so in stiffness values for JRO were observed. The change in environmental conditions was pointed as the reason for this variation within the four-year monitoring period.

Extracting structural properties from identified modal parameters is another challenging issue. Many structural property extraction methods were developed. These properties are used for updating the initial finite element models as well as for condition assessment of the structure.

Levin and Lieven [23] demonstrated a new finite element model updating method based on Neural Network (NN). Results from a set of finite element models which were generated by altering initial finite element model were used for training the neural network. This trained neural network contains the relation between change of model properties and change of modal parameters. Afterwards modal parameters identified from experimental data were simulated in the NN. This process results in adjustment coefficients of structural properties of initial model. New adjustment coefficients were applied to the initial finite element model and an iterative procedure was followed until the finite element model properties converged. This NN based updating method was also validated by a simulated test using a two-dimensional cantilever beam. Unlike the previous methods, the proposed method is resistant to experimental noise and works with limited number of identified modal parameters.

Calcada *et al.* [24] conducted a study on developing a numerical model to simulate dynamic responses of vehicle-bridge system. Monte Carlo simulation was used for dynamic amplification factor evaluation. A finite element vehicle-bridge system was constructed and 32 different simulations. Each simulations were prepared by changing road roughness, vehicle speed and traffic flow in terms of number of vehicles, distance between vehicles and passing directions. Finally, obtained results were compared with real case results and then numerical model was updated and validated.

Variation in identified modal parameters of different data sets is a critical problem in structural identification. Increase in the amount of variation causes decrease in accuracy and reliability of condition assessment process for structures. There are many studies indicating this variation problem. Some of which are given below.

Peeters and DeRoeck [25] conducted a study on separating abnormal changes from normal changes in the dynamic behavior of structures. While normal changes were described as changes due to environmental effects such as temperature, wind, humidity, abnormal changes were associated with stiffness loss due to damage. In this study a three span classical box girder bridge was instrumented with 49 sensors to collect environmental parameters besides acceleration sensors. An automatic modal analysis methodology based

on time domain stochastic subspace identification technique was proposed for the estimation of modal parameters. A black-box autoregressive model was constructed by only considering temperature for mapping the relation between identified modal frequencies and environmental effects for healthy structure. It was shown that there was no relation between other environmental effects except temperature and modal frequencies.

Sohn *et al*. [26] conducted a study on predicting changes in modal parameters due to environmental effects. A linear adaptive model was constructed to identify effects of temperature on modal parameters. For demonstration of efficiency of linear adaptive filters, modal parameters identified with eigensystem realization algorithm from a seven span composite bridge were used. While one data set was used for adaptive filter training, others were used for validation. A more comprehensive well-controlled study considering a wider temperature range was suggested to fully validate this linear model.

SHM of structures under the effect of measurable excitations gives more reliable identification results; however, excitation sources cannot be always controllable, quantifiable or easily measurable for bridges. In this case many assumptions and representations were developed for traffic loads under the topic of "Vehicle-Bridge Interaction" (VBI).

Green and Cebon [27] conducted a study on importance of VBI with heavy vehicles and bridges. A new method was demonstrated by using a single degree of freedom sprung mass vehicle model travelling on a simply supported beam. Afterwards a parametric study was conducted with six different parameters which are speed, bump height, the ratios of frequency, mass, vehicle damping and bridge damping. The most important parameters were determined as speed, frequency and initial vehicle excitation. Large mass ratios also resulted in important interaction at high speed. Bridge and vehicle damping became also important when the ratio was near to unity. Lastly, this study recommended using extended vehicle models and a systematic study on the effects of bridge surface roughness.

Awall *et al*. [28] carried out a Parametric Study on Bridge-vehicle Interaction Dynamics. In this study, extended three-dimensional finite element interaction analyses

were conducted parametrically. It was concluded that dynamic amplification varies with different parameters such as speed and road roughness.

An efficient and accurate vehicle-bridge interaction model for railway bridges under high-speed trains was developed by Yang and Yau [29]. The train was modeled as a series of sprung mass system. Roughness of the beam was considered for dynamic interaction. This constructed vehicle-bridge interaction model was also verified with numerical examples.

1.4. Statement of the Problem and Objectives

It was shown that a variation problem in identified modal parameters of real-world structures still exists. In some studies [25, 26] which did not consider the input excitation, the change in the temperature was indicated as one of the reasons for variations. Besides, in many studies [24, 27] change in some dynamic properties was investigated by parametric studies including different parameters such as speed, damping ratios, mass ratios, etc. However, in those studies identification of real-world structures are not considered. Finally, in a long term monitoring study [30], a fluctuation up to 10% in identified modal parameters from traffic-induced vibration measurements was observed under the same environmental conditions over the same period.

Furthermore, condition assessment of the structures is mainly based on conditions of the structural elements. Conditions of the structural elements are extracted by using identified modal parameters. Thus, variations in modal parameters results in variations in extracted structural properties.

Uncertainties of the VBI make it difficult to precisely identify modal parameters of bridges under traffic excitation. Assumption of taking the traffic input source as uncorrelated white noise is mostly used in identification processes. Although this assumption is very consistent for many measured data sets, a big amount of variation exists in the studies.

The main objective of this study is presenting the possible reasons of the variation in identified modal parameters of bridges. It is aimed to identify modal parameters, then, corresponding structural properties and examine the effects of static mass, correlated input and speed parameter of moving loads on identified modal parameters of bridges.

1.5. Scope and Outline

This Chapter contains a general introduction of this study including motivation of SHM, a literature review, statement of the problem, objectives and scope.

In Chapter 2, basic information about system identification concept is presented. Some system identification techniques related to this study are pointed and a detailed description of the FDD method is given. The Jamboree Road Overcrossing (JRO) is analyzed as a case study. Traffic-induced vibration measurements from JRO are analyzed with FDD method and identified modal parameters and variations were exhibited.

In Chapter 3, a finite element model for JRO is constructed. Moving load, static mass and modal analyses are prepared within this model. The concept of extracting structural properties by using NN is briefly explained. A radial basis NN is created and a set of input output data of finite element models of JRO which was created from previous study [30] is used for training the NN. Finally, identified modal parameters given in chapter two are simulated with trained NN and structural properties of JRO are extracted.

In Chapter 4, the effects of traffic loading on modal parameters are investigated by moving load and delayed white noise load analysis. The effect of static mass is also considered separately. Effects of indicated analysis on variation are demonstrated.

In the final chapter, a summary of findings and recommendations for further studies are listed.

2. STRUCTURAL IDENTIFICAION

In this chapter, basic information about system identification concept and some of the identification techniques are presented. FDD method is described in details and used for identification of modal frequencies and corresponding mode shapes of the JRO. Finally, variations in identified modal parameters and possible reasons are exhibited.

2.1. System Identification

The process of determining or updating the properties of a model of a physical dynamic system by using measured data is called system identification. The primary objective of the system identification is to determine the current system properties quantitatively. Basically, there are three main steps in system identification process:

- Developing a model of the system
- Collecting data from real system
- Performing suitable system identification methodologies

The first step of system identification process is developing an approximate mathematical model of the physical dynamic system. In structural engineering, finite element models are often used. This model should represent the behavior of the real system approximately. There is no prior knowledge on the behavior of the real system in many types of identification problems. There do not exist governing equations or inequalities to represent the systems. In this case, implicit algorithms or equations are mostly used in identification processes as models; however, in some engineering problems, prior knowledge about the system may exist. Moreover, preliminary models for systems are present as design models in many engineering applications.

The second step of system identification process is collecting data from physical dynamic system. To describe a system as a dynamic system, it should show changes in the state of the system in response to external effects. There is a distinct relation between

inputs and outputs of the system. This relation directly stems from system properties. Some basic data should be collected from the response of the structure in order to represent its motion under corresponding excitations. Acceleration or displacement response of the structure and the data of the excitation source are the most crucial ones of these data sets. Many other observations such as strain and temperature data collection can also be done from different locations of the system. Increasing the number of observation points and types makes identification results more accurate.

Noise can be described as unwanted electrical disturbances generated in the measurement devices by themselves or nearby external electrical devices. Although all the measured data have some amount of noise, there are effective analysis methods to decrease the inaccuracies of the results due to noise. A generic representation of a dynamic system including noise is given in Figure 2.1.

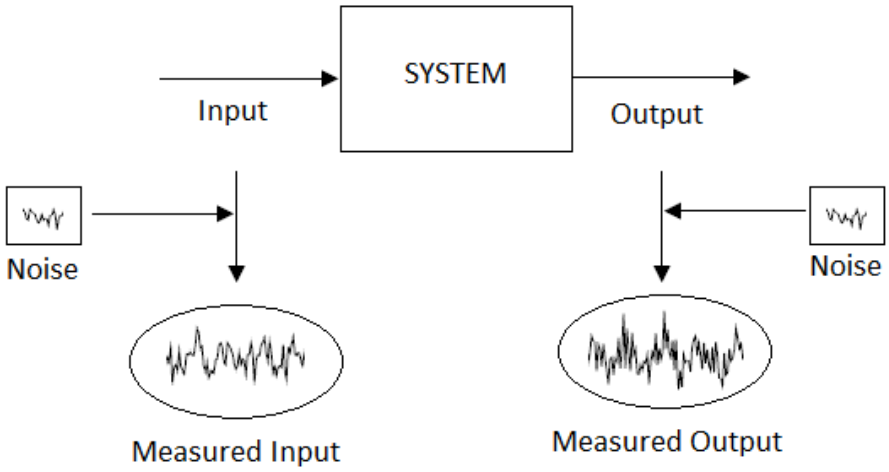

Figure 2.1. Visualization of a dynamic system.

The third step of system identification process is performing suitable system identification methodologies to identify system properties. During the last fifty years or so, many researchers have put substantial effort on developing reliable identification methods for structures. Identification methodologies could be categorized into two groups in terms of the domain of the analyzed data: time domain and frequency domain system identification. After the development of the fast Fourier transform algorithm, processing of the measured data became much faster and the development of computer technology

makes it a fundamental tool in structural identification methodologies. However, problems related to frequency resolution and leakage prompt researchers to work on time domain alternatives [31]. During the last decade, with the help of computational improvements, problems are being reduced for both domains.

Many methods have been developed for effective system identification process up until now. Maia and Silva [31] give basic explanations for many of these methods as listed below. Time domain identification methods:

- The complex exponential method
- The least-squares complex exponential method
- The polyreference complex exponential method
- The Ibrahim Time Domain method (ITD)
- The Eigensystem Realization Algorithm (ERA)
- The Autoregressive Moving-Average Method (ARMA)
- The direct system parameter identification method
- Many other identification methods driven from ARMA, ERA and ITD

Frequency domain identification methods:

- Peak picking method
- The Circle fitting method
- Ewins-Gleeson method
- The complex exponential frequency domain method
- Frequency domain decomposition method
- The rational fraction polynomial method
- The global rational fraction polynomial method
- The polyreference frequency domain method

With the use of these system identification methods, many specific structural system identification methodologies were demonstrated.

2.2. Output-Only Structural System Identification Methods

Structural system identification can be separated into two main groups according to the available data type:

- Input-output structural system identification
- Output-only structural system identification

Structural system identification process of an input-output system results in more accurate identified system parameters. However, unlike the laboratory experiments, the excitation sources cannot be always controllable, quantifiable or easily measurable for real-world structures under the service loads. For this reason output-only structural system identification methods are the most useful methods for bridges as well as for many other real-world structures.

Main advantages of using output-only structural system identification methods instead of other methodologies for bridges could be summarized as follows:

- It does not interrupt traffic even in the instrumentation step before measurements.
- It provides real dynamic characteristics of the bridge due to its normal service loads.
- It can be performed by smaller and user friendly devices instead of bigger special test setups such as shakers, impulse hammers, and test trucks.
- It can be controlled worldwide by a remote control system after instrumentation.
- It can be performed continuously, periodically or automatically by defining triggering levels.

Many output-only structural system identification methods were developed and demonstrated by researchers. These are basically the natural excitation technique [32, 33], the subspace decomposition [34], stochastic subspace identification [35], random decrement [19, 36], Ibrahim time domain method [37], peak picking method [38], Frequency Domain Decomposition (FDD) [39, 20], circle fitting method [40] and many ARMA models. Due to its simplicity, FDD method is the most popular identification

method for bridges. The common assumption of all these output-only methods is considering the input as uncorrelated white noise.

2.2.1. Frequency Domain Decomposition

The Frequency Domain Decomposition (FDD) method was firstly developed by Brincker *et al*. [39]. This method is mainly based on complex mode indication function technique that was introduced by Shih *et al*. [41].

When using the FDD method, in order to obtain consistent results, three main requirements should be satisfied:

- Input should be assumed as uncorrelated white noise.
- Structure should be lightly damped.
- Close modes should be orthogonal.

The FDD method is very similar to other frequency domain techniques. These frequency domain techniques are based on the calculation of spectral density matrices of the measured output data by Fourier transformation. In those techniques modal frequencies are determined by picking the peaks in spectral density diagrams.

However, in the FDD method spectral density matrices of data are decomposed into a set of single degree of freedom system for each frequency by using Singular Value Decomposition (SVD). SVD approach is the main advantage of FDD method.

On the other hand, the main disadvantage of FDD methods is the uncertainty in damping estimation. Time domain techniques give more accurate estimations for damping ratio; however, damping ratio is not considered in this study.

The relation between the immeasurable input $X(t)$ and measured output $Y(t)$ can be described in the form of spectral densities:

$$S_{YY}(\omega) = H(\omega)S_{XX}(\omega)H^H(\omega) \tag{2.1}$$

where $S_{YY}(\omega)$ is the Power Spectral Density (PSD) matrix of the measured responses, $S_{XX}(\omega)$ is the PSD matrix of the inputs, $H(\omega)$ is the Frequency Response Function (FRF) matrix and superscript ^{H} denotes the Hermitian (complex conjugate transpose) of the matrix. By modal decomposition FRF can be written as:

$$H(\omega) = \Phi\Lambda(\omega)\Phi^T \tag{2.2}$$

where Φ is the unitary mode shape matrix and $\Lambda(\omega)$ is a diagonal matrix which contains the transfer functions for each mode. The inputs are usually unknown for experimental modal analysis of real-world structures. Assumption of defining the input as uncorrelated white noise is the main criteria for FDD method; therefore, PSD matrix of the inputs can be written as:

$$S_{XX}(\omega) = kI \tag{2.3}$$

Plugging Equation 2.2 and 2.3 into Equation 2.1 gives:

$$S_{YY}(\omega) = \left[\Phi\Lambda(\omega)\Phi^T\right][\,kI\,]\left[\Phi\Lambda(\omega)\Phi^T\right]^H \tag{2.4}$$

Then PSD matrix of the measured responses takes the final form of:

$$S_{YY}(\omega) = k\Phi\Lambda(\omega)\Lambda^H(\omega)\Phi^T \tag{2.5}$$

By applying the singular value decomposition, the spectral density matrix $S_{YY}(\omega)$ is decomposed into:

$$S_{YY}(\omega) = U(\omega)\sum(\omega)U^H(\omega) \tag{2.6}$$

where $U(\omega)$ is a unitary matrix containing singular vectors, $\sum(\omega)$ is a diagonal matrix involving the singular values. By comparing Equation 2.6 with Equation 2.5 the mode

shapes are given by singular vector $U(\omega)$ which is corresponding to the related singular values $\sum(\omega)$.

2.3. Jamboree Road Overcrossing

The Jamboree Road Overcrossing (JRO) is located in Irvine, CA, US. It is a three-span pre-stressed (post-tensioned) continuous box girder bridge. The JRO was designed and constructed in accordance with American Association of State Highway and Transportation Officials (AASHTO) Standards. The construction of this bridge was completed in 2001. A satellite view of the JRO is given in Figure 2.2.



Figure 2.2. The satellite view of the JRO [42].

The total length of the bridge is 111.56 m. It has three spans which are 34.75, 46.33 and 30.48 m long, respectively. The JRO is supported on two columns and two abutments at each side. The connections between abutments and superstructure were designed as sliding bearings which are supported with elastomeric bearings. In plan view, abutment 4 is skewed at 30° from transverse direction.

The columns are a combination of two circular columns intersecting each other. The width of the column, which is also the diameter of the circular shape, is 1.67 m and the total depth of the columns is 2.51 m. While abutments are supported with sliding bearings, columns are continuous with the superstructure. Each columns and abutments have reinforced concrete pad footings supported on piles. Plan and side views of the bridge drawings are given in Figure 2.3.

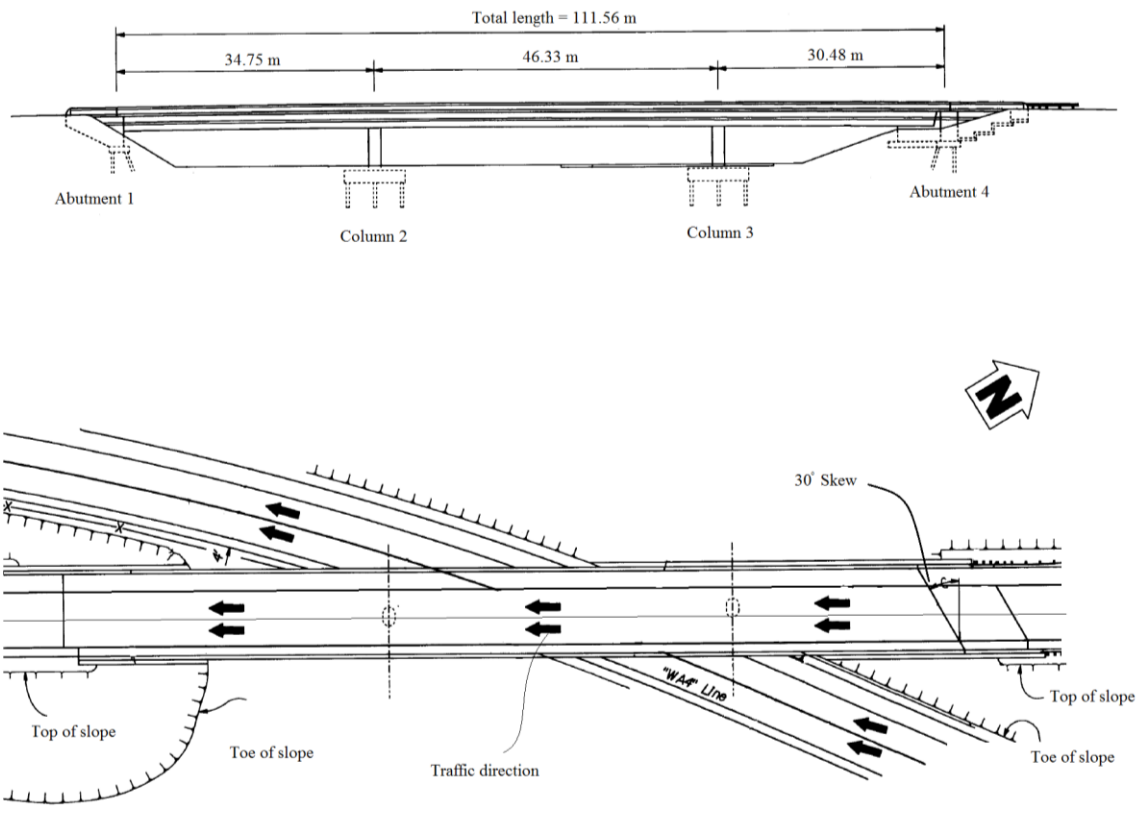

Figure 2.3. Plan and side views of the JRO [43].

2.3.1. Instrumentation of the JRO

A 16 channel data recorder which has a sampling frequency of 100Hz was used in this study. This amount of sampling frequency allows analyzing the structure within the range of 0-50 Hz, which is sufficient to identify modal frequencies of many types of structures including typical highway bridges. The monitoring system was configured as automatic recorder with a triggering level of 0.002 g from related sensors at the base of the column three. Once triggered, the data recorder automatically records 60 seconds data and

a solar backup power system was established to prevent power failure for data recorder and sensors.

Uniaxial, biaxial, and triaxial force-balance servo-type accelerometers which have a maximum noise level of 0.00067 g were installed on the bridge by a research group of University of California, Irvine (UCI) after the bridge was opened to traffic. Figure 2.4 shows the layout of the sensor locations at the JRO. To minimize the torsional effect of the superstructure, sensors were placed along the center line of the bottom of the girder.

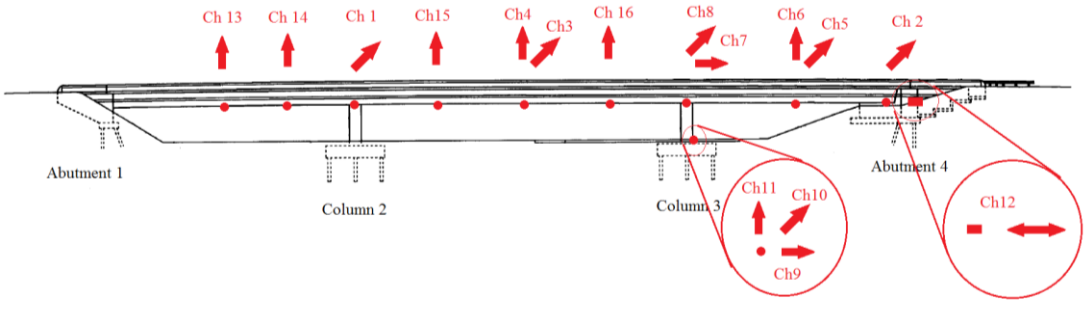

Figure 2.4. The layout of the sensors [43].

At the beginning, 15 of the 16 channels of the data recorder were used for acceleration sensors which are located on the superstructure and also on the top and bottom of column three. The remaining channel was planned to be used for measuring the change in displacement between superstructure and abutment four due to shortening, creep, shrinkage and also seismic excitations. However, displacement sensor (in channel 12) and one of the acceleration sensors (in channel 16) became malfunctioned after the bridge was opened to traffic, so the number of channels reduced to 14. After 2006 channel 15 also malfunctioned.

A wireless data transmitting system using point-to-point antennas was installed for remote control. Wireless antenna and solar panels of the backup power system can be seen in Figure 2.5. By implementation of this setup, data acquisition system can be easily controlled within the research center located at the UCI which is approximately 10 km away from the JRO site. Measured data, which is also temporarily stored at the site, was transmitted through this wireless system to the research center server. By the use of this

server, data acquisition system can be controlled worldwide through the internet and this wireless transmitting system is also monitoring the JRO monitoring system.



Figure 2.5. Wireless antenna and solar panels [44].

2.3.2. Acceleration Data of the JRO

There are six transverse, six vertical and two longitudinal acceleration sensors and all sensors capture simultaneous data; however, in this study only vertical acceleration data of the superstructure is considered. Channel 4, 6, 13, 14 and 15 are connected to the sensors located at spans and measure vertical excitation. A typical acceleration response at vertical sensor locations is shown in Figure 2.6. Red lines represents the arrival times of the vehicles to demonstrate time delays between the first and the other sensors.

Peak magnitudes of the data sets are varying from 0.005 to 0.040 g. This variation could result from varying vehicle mass, velocity and other external effects such as wind and vehicles passing under the bridge. Most of the cases, data sets consist of a combination of different peaks. This means that combination of different types of excitation sources results in a combination of different peak values in data sets.

Results of 1622 out of 1709 data were considered after the identification step. Eighty seven corrupted data sets were sorted out from the whole data by simply looking its mean and root mean square values.

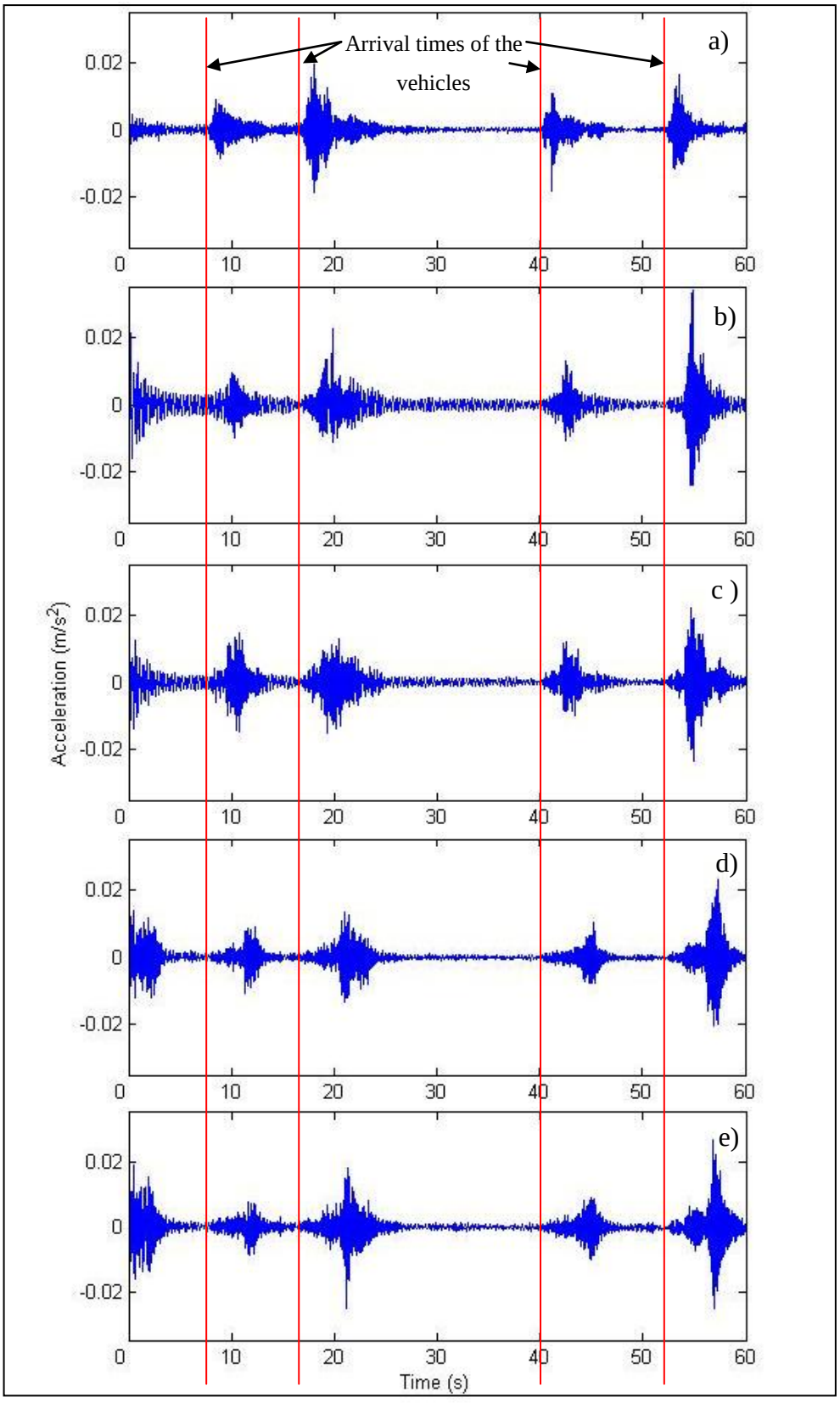

Figure 2.6. Typical acceleration responses of the channel (a) 6 (b) 4 (c) 15 (d) 14 (e) 13.

2.3.3. Identified Modal Parameters of the JRO

In this part, identified modal frequencies from 1622 traffic-induced vibration data are discussed. Because of the fact that traffic excitation input cannot be measurable, FDD method is used for identification of the JRO from these output-only data sets.

Each data set is 60 seconds long and sampled at 100 Hz. Number of fast Fourier transform was taken as 2048 that provides 0.025 Hz resolution for identification process. To decrease the effects of leakage, 2048 point hanning window is used with a 50% overlapping for each segment.

Figure 2.7 shows an acceleration response of channel six on 31st of May, 2002. A typical result of FDD application on this data set is shown in Figure 2.8. This plot shows the first singular values created by taking the SVD of the PSD matrices of the output data. The second singular values are approximately 100 times smaller than the first ones as seen in Figure 2.9; thus, the first singular values (eigenvalues) and corresponding eigenvectors are good enough to describe the whole matrix. Modal frequencies are determined as 2.88, 4.64, 6.10, 8.69 Hz, respectively, for this data set.

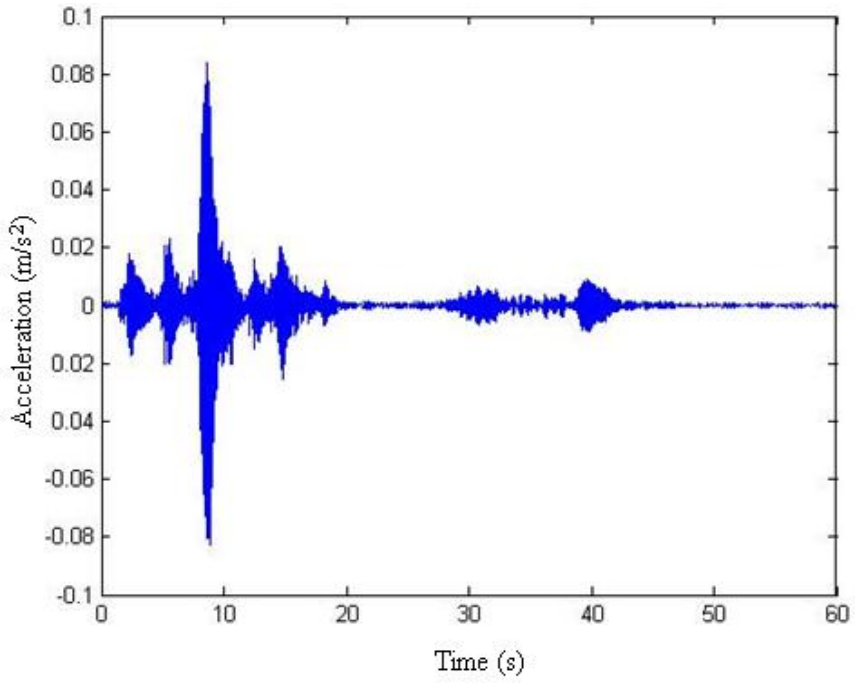

Figure 2.7. Acceleration response of channel 6 on 31st of May, 2002.

By examining some more data, it can be seen that modal frequencies are well separated that a predefined numeric interval around these peaks could be given for searching and selecting the peak values from the plot of first singular values automatically.

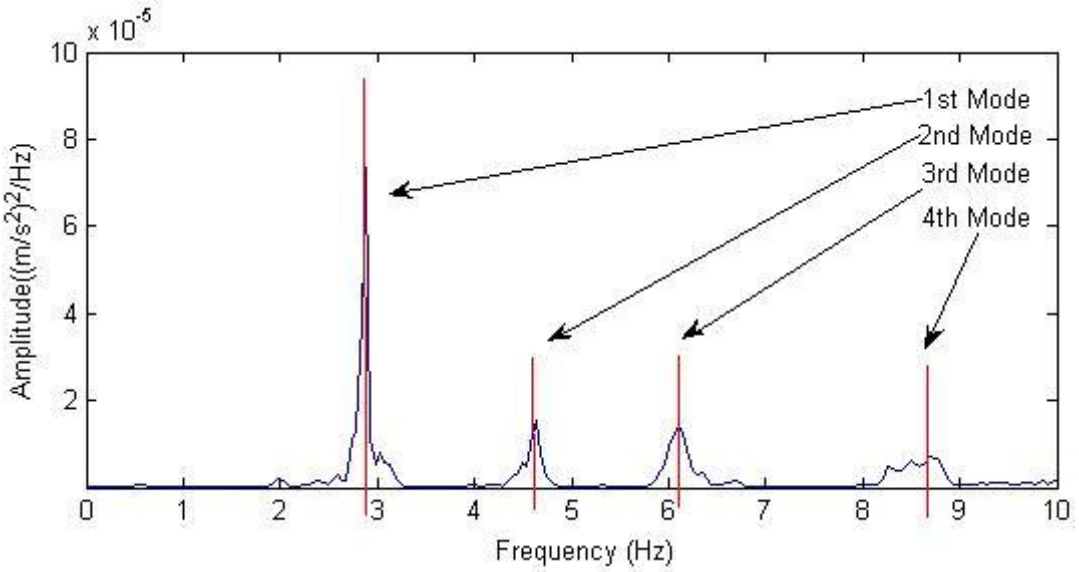

Figure 2.8. First singular values of the PSD matrice and peaks.

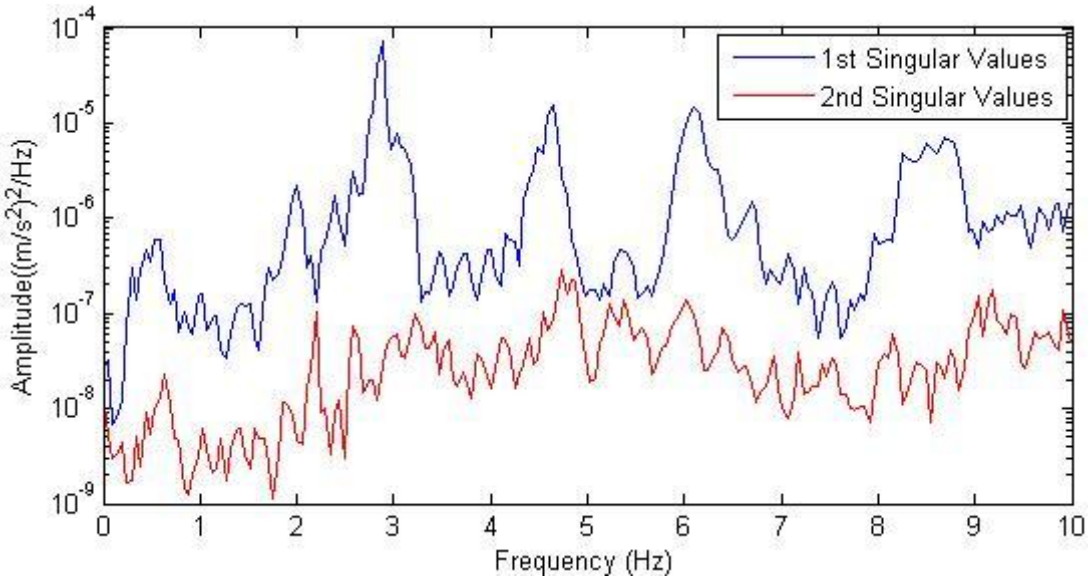

Figure 2.9. First and second singular values of the PSD matrice.

All in all, first four modal frequencies from 1622 data sets are identified. The identified mode shapes and modal frequencies are plotted in Figure 2.10 and Figure 2.11,

respectively. The intervals of identified modal frequencies and the comparison of these values with previous studies [45] are given in Table 2.1.

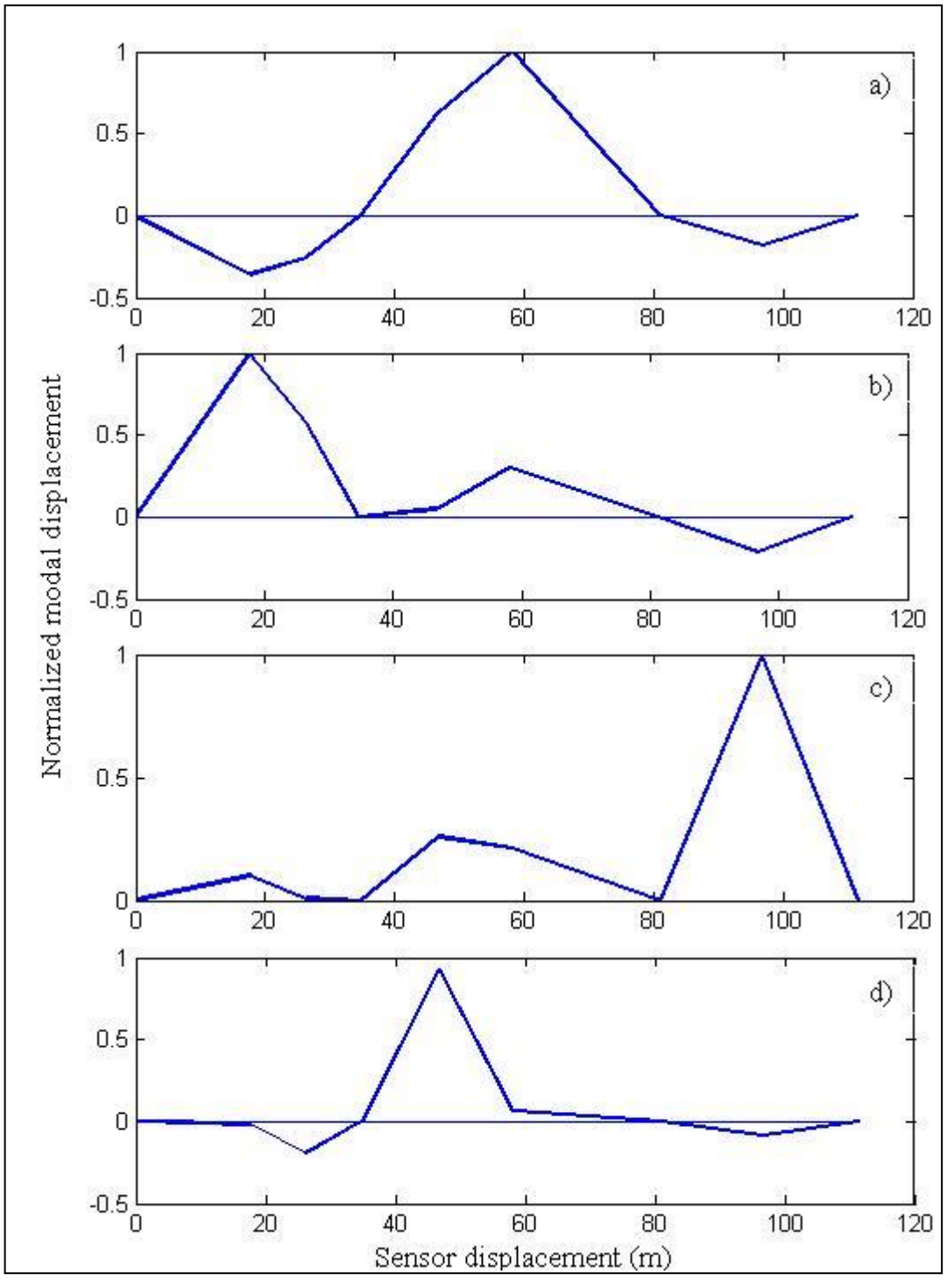

Figure 2.10. Identified mode shapes of the JRO corresponding to the (a) first (b) second (c) third (d) fourth mode.

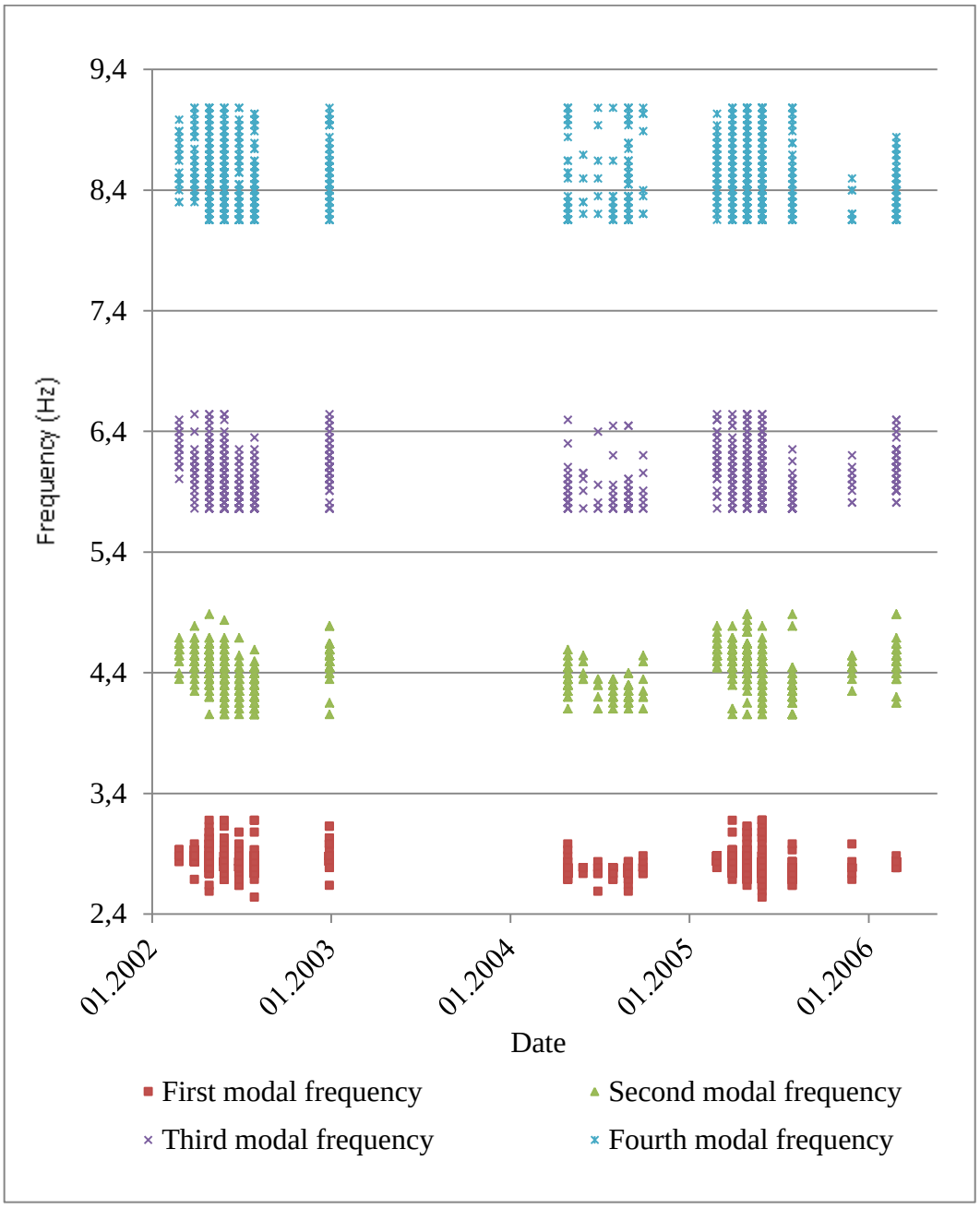

Figure 2.11. First four identified modal frequencies of the JRO.

Table 2.1. Identified modal frequencies of the JRO by different authors.

Authors	Number of data sets	Identified Modal Frequencies (Hz)			
		1st	2nd	3rd	4th
Feng et al. (2004)	82	2.95	3.98	4.64	6.25
Soyoz (2007)	1707	2.60-3.20	4.10-4.90	5.80-6.60	8.20-9.10
Gomez (2011)	1600	2.78-2.93	4.44-4.54	N/A	N/A
Celenli (2012)	1622	2.54-3.17	4.05-4.88	5.76-6.54	8.15-9.08

2.4. Variation in Identified Modal Parameters

First four modal frequencies are identified with frequency domain decomposition method and a variation from 5% to 10% was observed. Figure 2.12 shows the identified modal frequencies with the amounts of variation. The reasons for this variation could be categorized into two main groups. The first group of reasons is related to the changes in environmental conditions. These are called environmental effects such as change in temperature and moisture. Peeters and DeRoeck [25] reported that with the increasing temperature Young's modulus of concrete decreases. This decrease directly results in a decrease in stiffnesses of structural elements. Finally, decrease in stiffnesses of structural elements leads to a decrease in modal frequencies. In this one-year long-term monitoring study on Z24 Bridge, a dramatic change in modal frequencies under the effect of temperature change from -10 C to +40 C was shown.

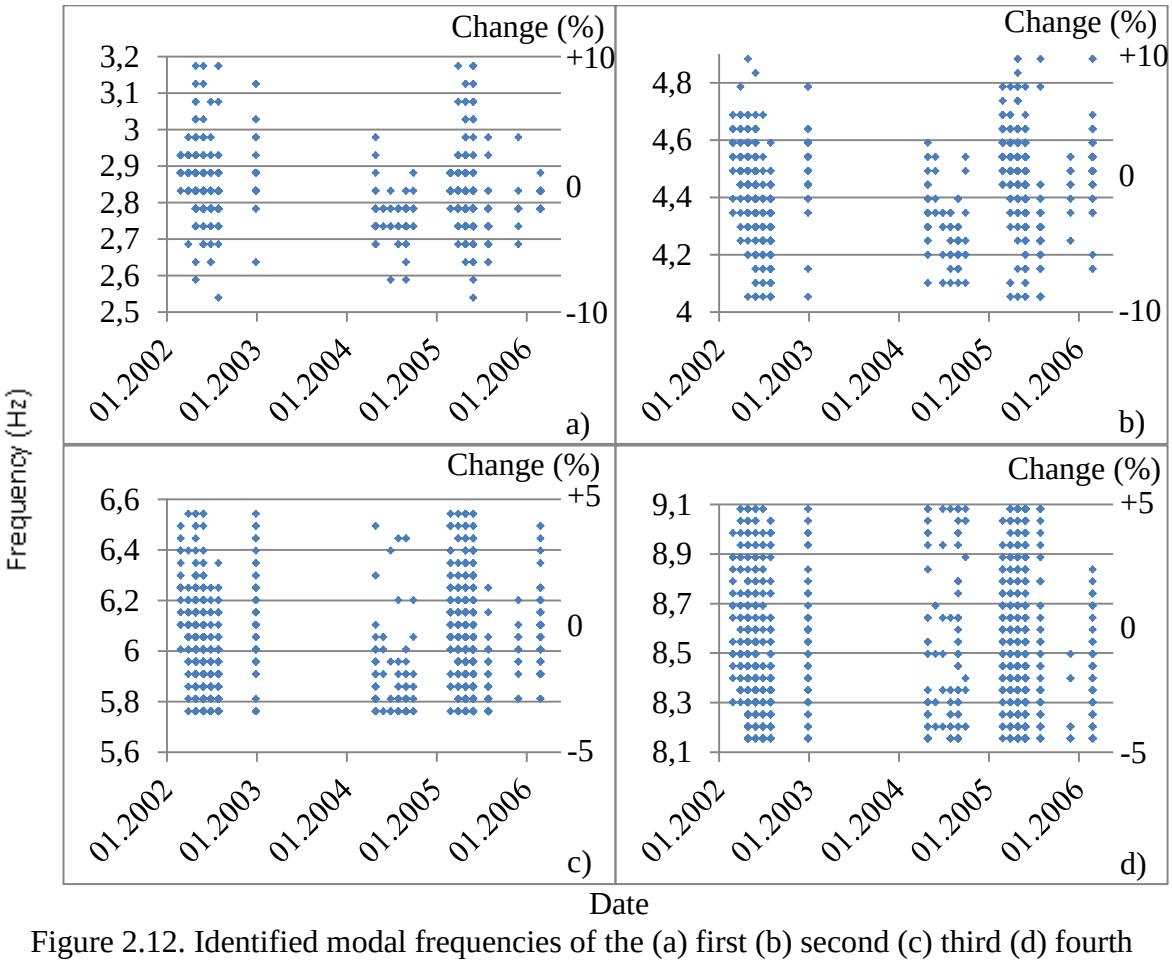

Figure 2.12. Identified modal frequencies of the (a) first (b) second (c) third (d) fourth mode.

Temperature information was not stored in data sets of JRO; however, data sets could be divided into two separate groups for winter and summer seasons. Soyoz *et al*. [30] noted that in the city of Irvine, average temperatures in November to April and May to October periods are almost constant. It was shown that identified modal frequencies are decreasing year by year both for winter and summer seasons. Aging of the concrete was pointed as the main reason of the decrease in modal frequencies in long-term analyses.

Besides, a big variation was observed between two consecutive data sets in the same season. Variation in modal frequencies seems to be independent from the change in environmental conditions since maximum variation may occur within a minute. Figure 2.13 shows the change in the first identified modal frequency between two consecutive data recorded on April 25, 2002 from 08:43:39 to 09:23:12. Thus, it can be stated that environmental effects are not the main reason for variations in identified modal parameters of JRO.

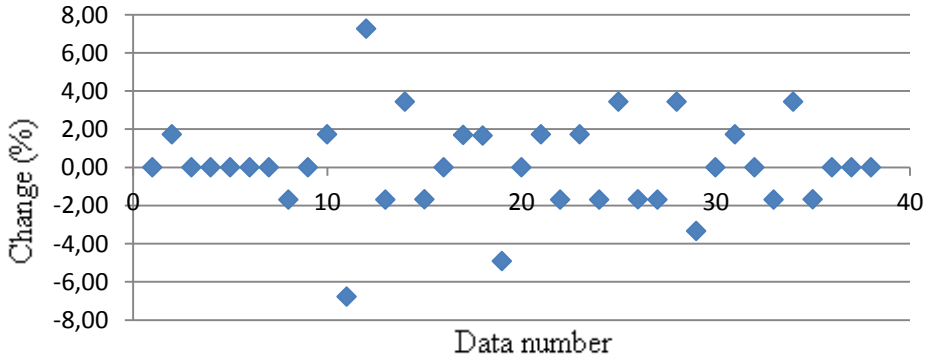

Figure 2.13. Changes between the first modal frequencies identified from consecutive data sets.

The second group of reasons is related to the change in input characteristics. Vehicle mass, velocity, suspension type, wind and other parameters affecting the vehicle-bridge interaction could cause dramatic variations in identified modal frequencies. Many parametric studies [27-29] were conducted to identify these reasons. In Chapter 4, effects of static mass, correlated input and speed parameter of moving loads on identified modal parameters of bridges are discussed.

2.4.1. Discussion in Identification of the Data in Segments.

In order to observe the effect of different types of acceleration peaks, data sets are also analyzed by splitting the data into segments. A test window is created with 2048 data point. This window is moved by 200 data point for each segmental analysis. By this means, identification of 19 segments of the data is carried out. Some of the segments are shown in Figure 2.14.

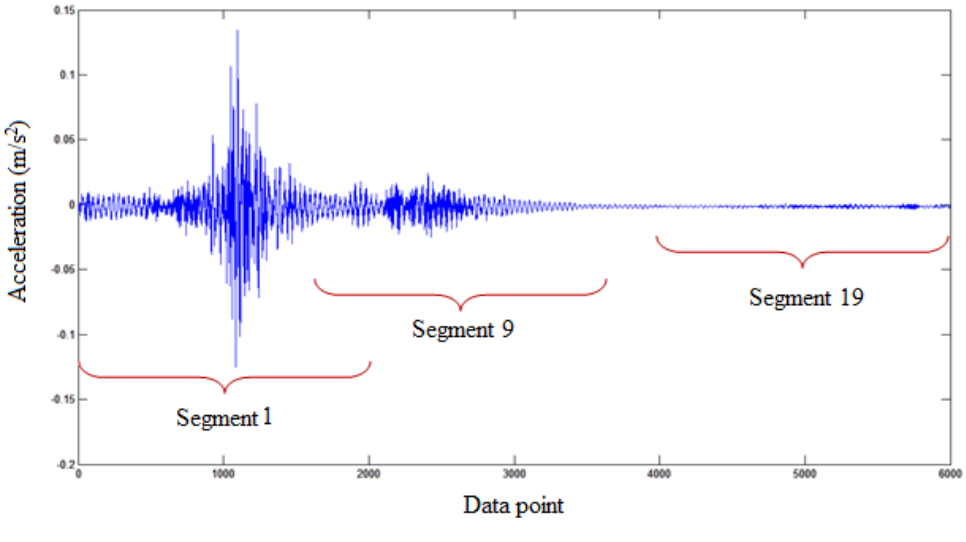

Figure 2.14. Identification of an acceleration data with different segments.

Identified first modal frequency of this data set is 3.08 Hz when the whole data is considered; however, when it is analyzed in segments, different segments give different frequency results as seen in the Figure 2.15.

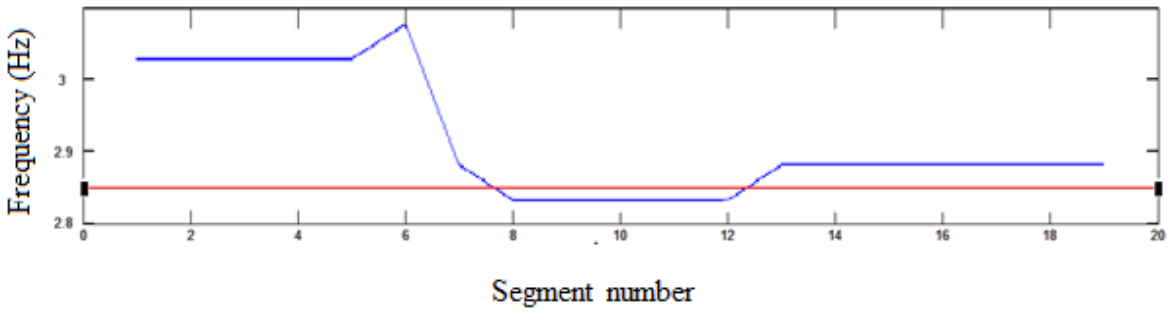

Figure 2.15. First modal frequencies identified from different segment.

High level of accelerations is expected due to the heavier vehicle loads. It is also expected that increase in mass results in decrease in modal frequencies; however, in this example, higher frequencies are identified from higher level accelerations.

This variation is valid for most of the data sets which caused a big amount of variation in identified modal frequencies. As a result, the characteristics of the acceleration output which is also stemming from the properties of the passing vehicle at that time, has a significant effect on the instant modal frequency.

3. FINITE ELEMENT MODEL AND STRUCTURAL PROPERTIES

3.1. General

The JRO is modeled by SAP2000 which is one of the structural analysis package programs. Moving load, static mass and modal analyses are conducted within this model. In this section construction of the initial model and results of modal analysis are presented. Structural parameter extraction from identified modal parameters of the bridge is also demonstrated. Results of the other analyses are given in Chapter 4.

3.2. Bridge Properties

Structural properties are the main components of a finite element model. From the design drawings [43], it is concluded that there are three basic structural elements for the JRO.

The most important structural element of this bridge is the box section girder. This study is interested in only vertical modes of the structure and these modes are primarily affected by the properties of superstructure which forms 86% of the whole structure. This section has a width of 12 meters and a depth of 1.9 meters.

The second important structural element is the full section girder. This section is designed for transmitting internal loads through supports; thus, this section is only used at column-deck and abutment-deck interaction locations.

The third main structural element is the column. Columns are a combination of two circular columns intersecting each other. The width of the column, which is also the diameter of the circular shape, is 1.67 m and the total depth of the columns is 2.51 m. Detailed technical drawings of these sections are shown in Figure 3.1.

The columns are not located at the longitudinal centerline of the deck as seen in the Figure 3.2. This off center situation, however, does not have any effect on vertical modes and frequencies which are the main objectives of this study.

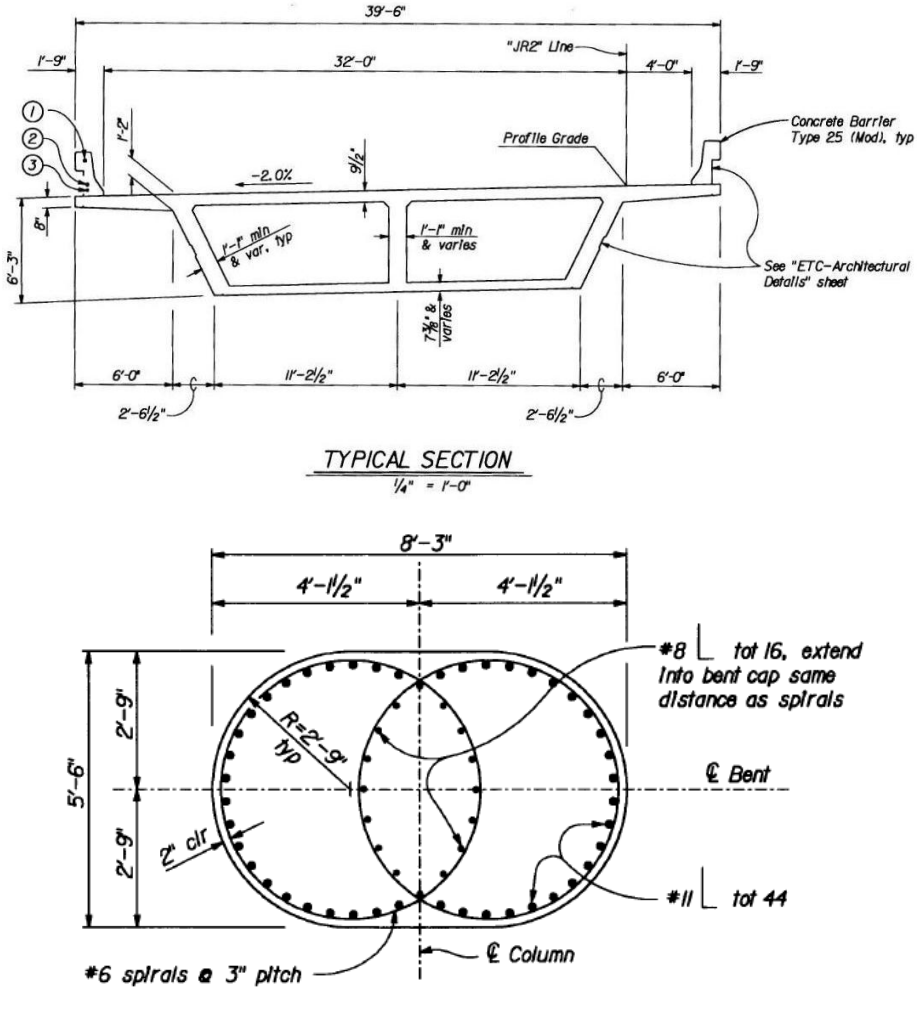

Figure 3.1. Technical drawings of box section girder and columns [43].

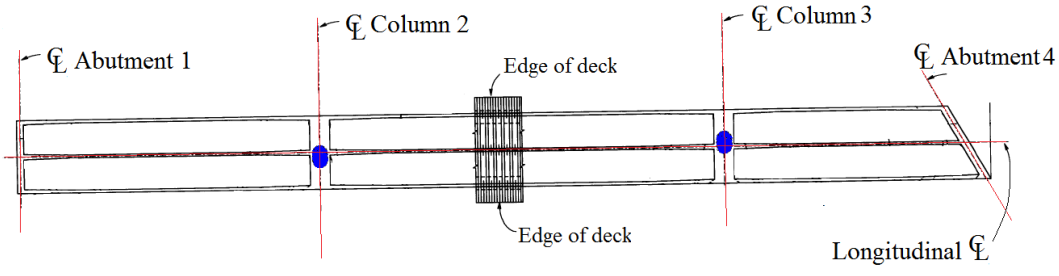

Figure 3.2. Plan view of the JRO from technical drawing [43].

By using the Section Builder interface of the SAP2000, these three structural elements are created exactly with the same dimensions of the design drawings. Section Builder automatically calculates the structural properties such as total area, unit weight, unit mass, moments of inertia, section modulus, plastic modulus and radius of gyration. The created box girder section with calculated properties is shown in Figure 3.3.

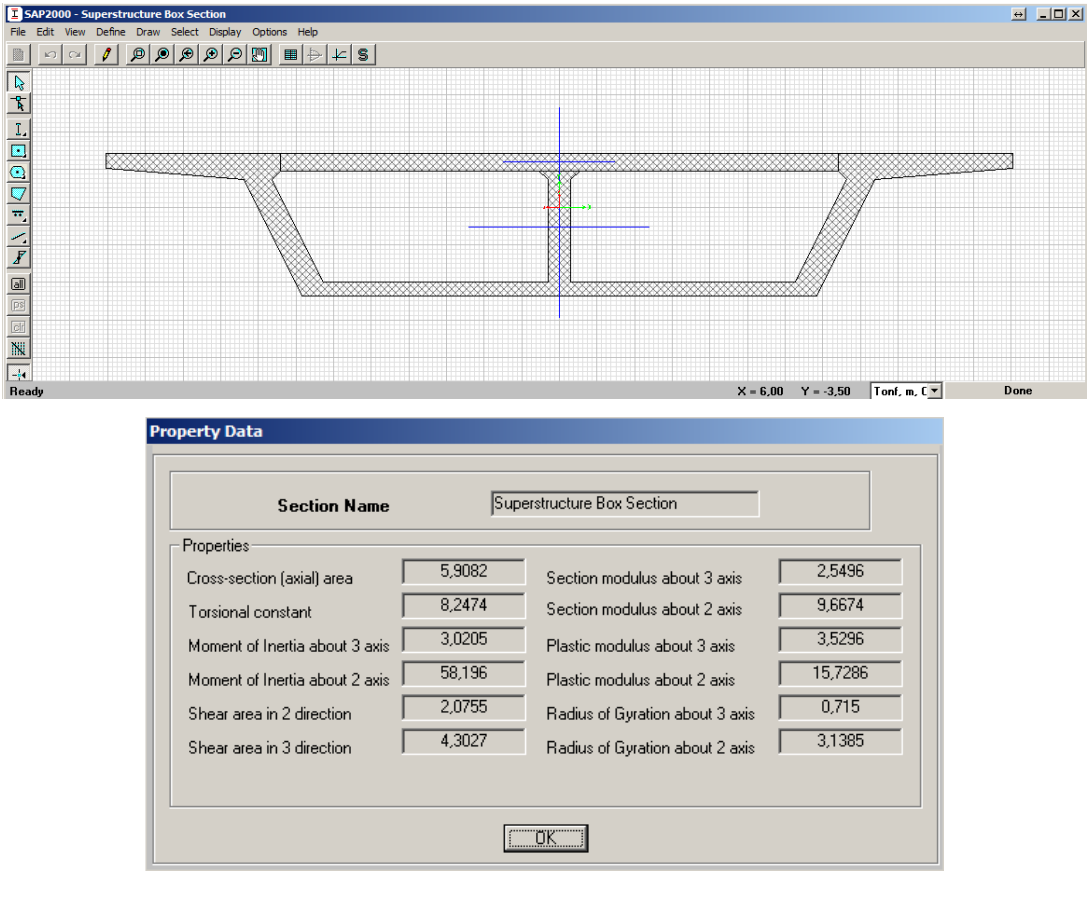

Figure 3.3. Box section girder element and properties.

Total length of the bridge is 111.56 m. There are three spans which are 34.75, 46.33 and 30.48 m long, respectively. All structural elements were constructed through section builder as line elements.

The end of the third span, supported at abutment four, is skewed at 30° from transverse direction. An assumption was carried out for this span that half-length of the skewed part was considered as a linear element for the whole skewed part.

3.3. Boundary Conditions and Soil Springs

The JRO is supported on two columns and two abutments at each side. While the connections between abutments and superstructure are designed as sliding bearings, columns are continuous with both the superstructure and footings. Each column and abutment has reinforced concrete pad footings supported on piles.

There is no single widely-accepted model for abutments, but in the report on seismic bridge design applications [46], FHWA gives soil spring models and calculations of these abutment springs, as seen in Figure 3.4, based on modulus of elasticity of backfill soil, height of the abutment, width of the abutment.

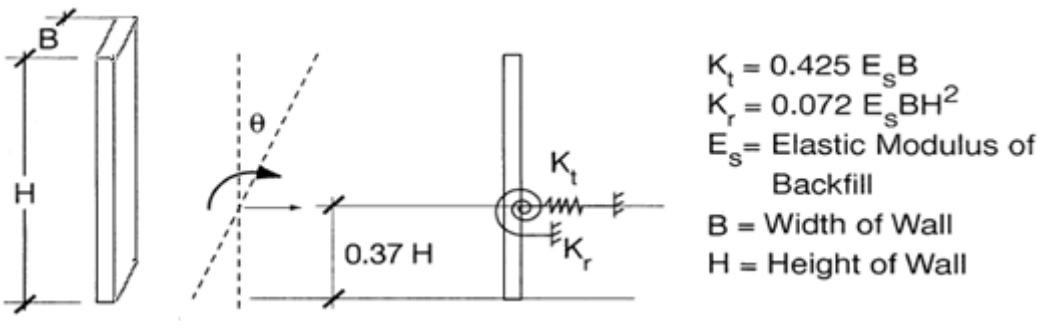

Figure 3.4. Soil spring calculations according to FHWA [46].

Figure 3.5 represents the finite element model with the constraints at supports. Columns were attached continuously with deck and fixed supports were used as footings. By using the FHWA design examples, longitudinal liner springs and rotational springs for abutments are calculated. Abutments are supported with sliding supports in longitudinal direction and also restricted with these soil springs. Displacement in vertical direction is also constrained.

All structural elements were created and all structural properties were determined. Structural properties of the superstructure elements, columns and abutments are listed in Table 3.1.

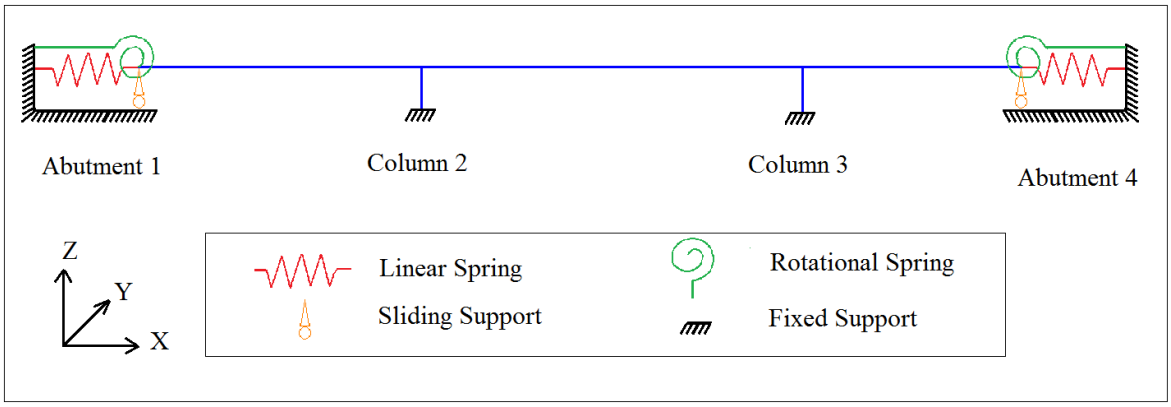

Figure 3.5. Constraints of the FEM of the JRO.

Table 3.1. Structural Properties of the FEM of the JRO.

Element	Area	Moment of inertia			Spring stiffness	
	Crossectional Area (m^2)	Ix (m^4)	Iy (m^4)	Iz (m^4)	Longitudinal (N/m)	Rotational (N.m/rad)
Superstructure Full Section	15.78	14.99	5.00	100.77	N/A	N/A
Superstructure Box Section	5.91	8.25	3.02	58.20	N/A	N/A
Column	3.86	2.19	0.81	1.75	N/A	N/A
Abutment	N/A	N/A	N/A	N/A	$2.00\ 10^8$	$0.07\ 10^8$

3.4. Modal Analysis Results

A 3D view of the created FEM of the JRO is given Figure 3.6. In this figure, box section girder element, full section girder element and columns are represented with yellow, orange and blue colors, respectively. Fixed supports and soil springs are also shown.

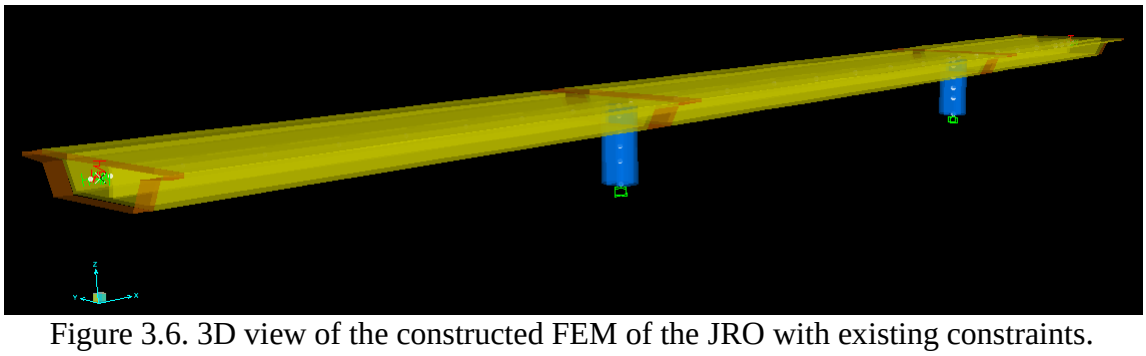

Figure 3.6. 3D view of the constructed FEM of the JRO with existing constraints.

Finite element models containing 40, 400, 4000 and 40000 structural elements are analyzed for convergence. Results are converged at FEM with 400 elements. The first five vertical mode shapes are given in Figure 3.7 and the first five modal frequencies were listed in Table 3.2.

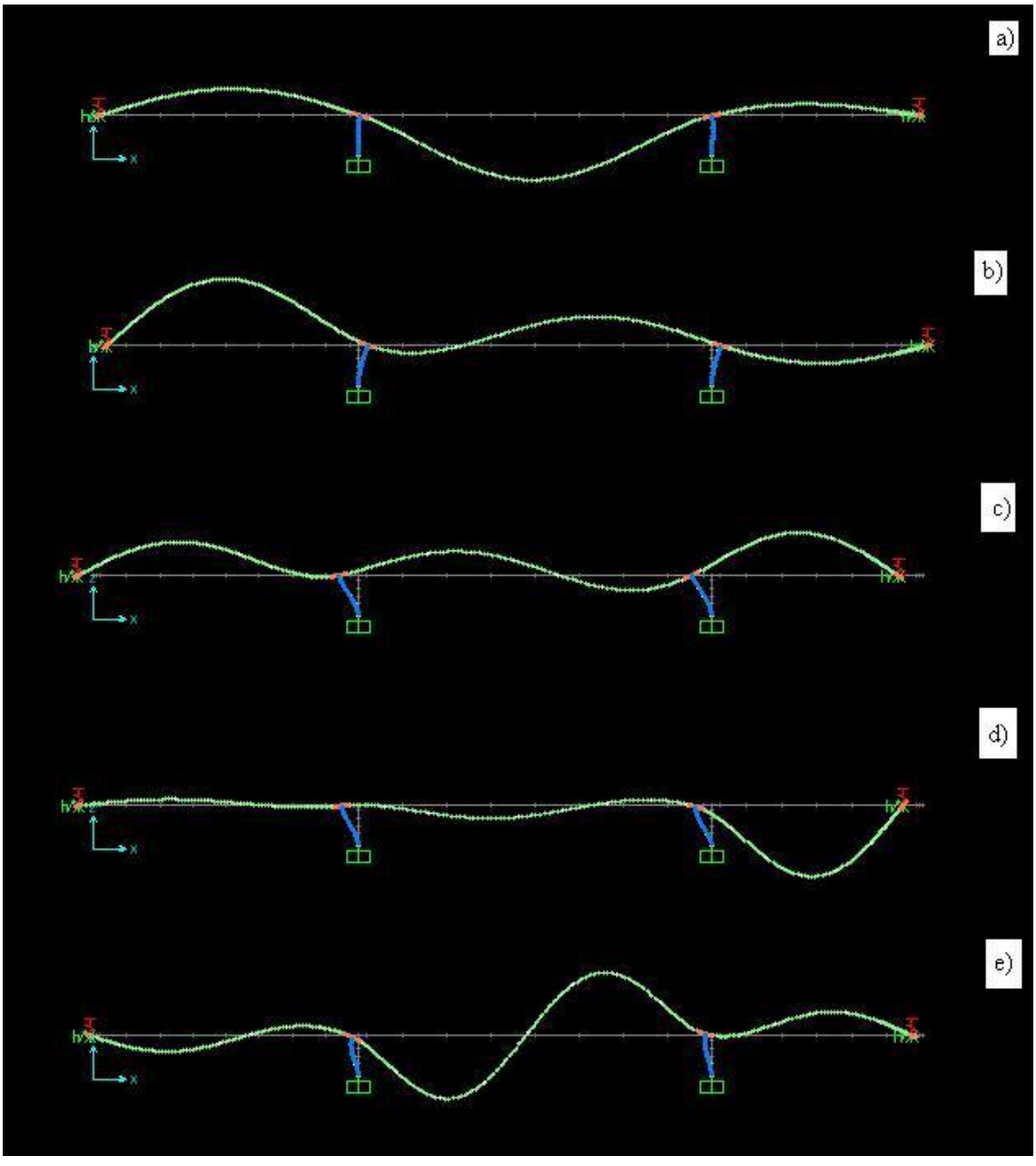

Figure 3.7. Mode shapes of the FEM of the JRO: (a) first (b) second (c) third (d) fourth (e) fifth mode.

Table 3.2. Modal frequencies of the FEM of the JRO.

Vibration modes	Modal frequencies (Hz)			
	FEM with 40 Elements	FEM with 400 Elements	FEM with 4000 Elements	FEM with 40000 Elements
First mode	2.84	2.83	2.83	2.83
Second mode	4.00	3.99	3.99	3.99
Third mode	5.43	5.42	5.42	5.42
Fourth mode	6.74	6.71	6.71	6.71
Fifth mode	8.88	8.85	8.85	8.85

3.5. Identification of Structural Properties

Many simulation methods were developed by researchers in order to extract structural properties from identified modal parameters such as Neural Network and Monte Carlo simulation based identification methods. These properties are used for updating the initial finite element models as well as for condition assessment of the structure.

There are no basic linear expressions or differential equations for real-world structures to express the relation between structural properties and modal parameters. The basic way to find modal parameters is to use finite element models. Results of the FEM analysis are changed based on the changes in structural properties. The model itself holds the relationship by iterative solutions of explicit relations.

Neural networks generate optimum relationships, within the predefined performance limits, between different input sets and different target sets even if they are irrelevant to each other. Generating this relation is only possible by training the network with numerous known input-target relations.

For structural identification, structural properties and corresponding modal parameter results of numerous finite element models generated by altering initial FEM are used for training the neural network. This trained neural network contains the relation between change of model properties and change of modal parameters. An example input-

target set, created from the FEM of JRO and descriptions of the structural property constants are given in Table 3.3 and Table 3.4, respectively.

Table 3.3. An example input-output set of FEM analyses of the JRO.

Set Number	Inputs of FEM						Outputs of FEM								
	Structural Properties Constants for finite element models						Modal Frequencies					1st Normalized Mode Shape			
	c1	c2	c3	c4	c5	c6	1st	2nd	3rd	4th	5th	1st Node	2nd Node	3d Node	4th Node
1	1	1	0.2	1	1	1	1.64	2.08	3.14	4.27	5.77	-0.26	-0.17	1.00	-0.09
2	1	1	0.4	1	1	1	2.11	2.77	4.06	5.43	6.80	-0.35	-0.24	1.00	-0.13
3	1	1	0.6	1	1	1	2.42	3.28	4.70	6.10	7.60	-0.39	-0.27	1.00	-0.15
4	1	1	0.8	1	1	1	2.67	3.69	5.18	6.53	8.33	-0.40	-0.29	1.00	-0.16
5	1	1	1	1	1	1	2.84	3.99	5.58	6.88	8.81	-0.41	-0.30	1.00	-0.17
6	1	1	1.2	1	1	1	3.06	4.33	5.79	7.20	9.55	-0.41	-0.30	1.00	-0.17
7	1	1	1.4	1	1	1	3.23	4.60	5.99	7.51	10.06	-0.41	-0.30	1.00	-0.17
8	1	1	1.6	1	1	1	3.34	4.83	6.14	7.81	10.52	-0.40	-0.30	1.00	-0.18
9	1	1	1.8	1	1	1	3.52	5.04	6.26	8.10	10.94	-0.40	-0.30	1.00	-0.18

Table 3.4. Structural property constants.

Structural properties constants for finite element models	
c1	Superstructure mass
c2	Column mass
c3	Superstructure stiffness
c4	Column stiffness
c5	Soil spring stiffness at A1
c6	Soil spring stiffness at A2

After the training process, identified modal parameters from experimental data are simulated in the trained networks. This process gives the adjustment coefficients of structural properties of the initial model. Figure 3.8 illustrates the extraction process of the structural properties coefficients.

Many neural network algorithms exist such as backpropagation, radial basis and time-delay neural networks. Generalized regression neural networks are a kind of radial basis networks that can be designed very quickly. In this study, a two-layer generalized regression neural network is created for extraction process as shown in Figure 3.9. A predefined input-target set [30] is used to train the neural network. This set was prepared by changing the superstructure mass, superstructure stiffness, column mass, column stiffness, soil spring stiffnesses of abutment one and abutment four.

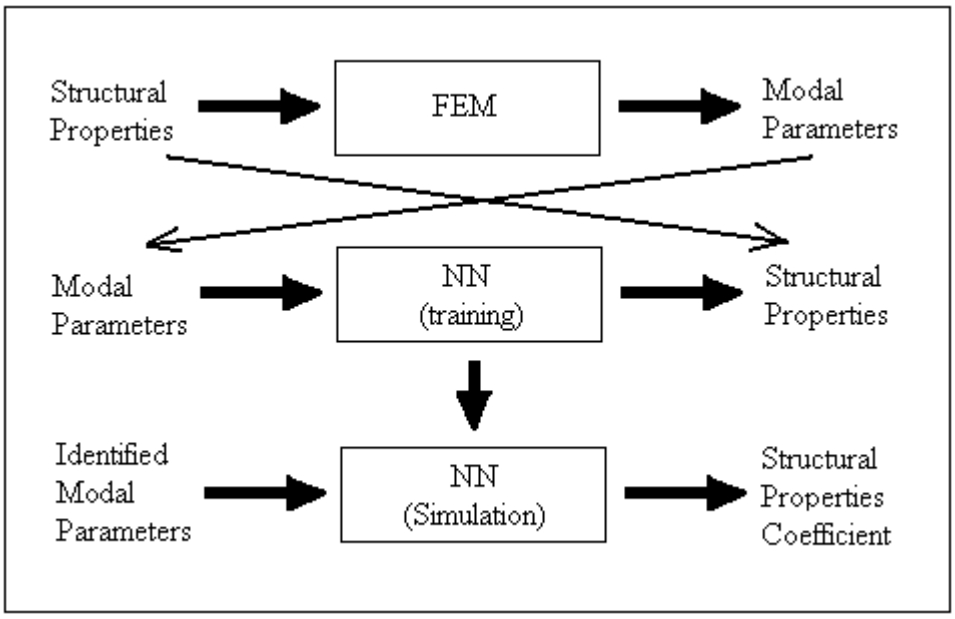

Figure 3.8. Extraction of structural properties by using NN.

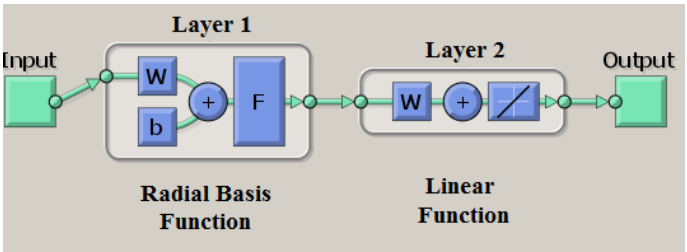

Figure 3.9. A two-layer radial basis NN.

After training the network, identified modal parameters of the JRO, given in Chapter 2, are simulated. Outputs of this simulation demonstrate the adjustment coefficients of structural properties of the initial model which are given in Figure 3.10.

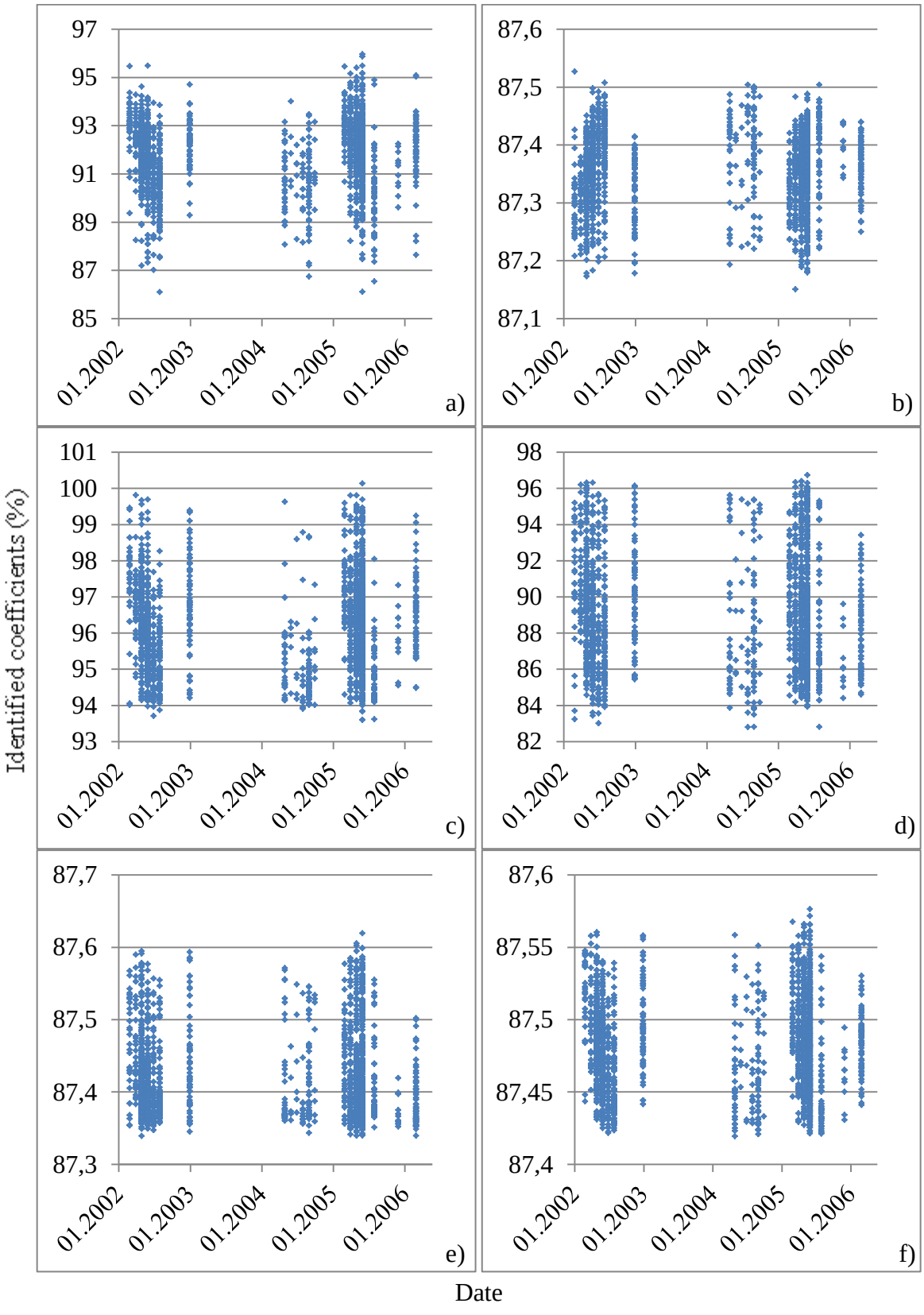

Figure 3.10. Identified coefficients for (a) superstructure mass (b) column mass (c) superstructure stiffness (d) column stiffness (e) soil spring at A1 (f) soil spring at A4.

A dramatic change in a short period is not expected in structural properties, especially in superstructure and column stiffness, unless damage occurs. However, column stiffness, superstructure mass and superstructure stiffness are found as 82% to 96%, 86% to 96% and 93% to 100% of the initial values, respectively. It is also demonstrated that change in vertical modal frequencies is directly related to change in these three structural properties.

Column mass and soil spring stiffnesses of each abutment are found as roughly 87% of the initial values with a negligible variation. Therefore, it is clearly seen that no relation exists between the variation in modal frequencies and these structural properties.

Some structural properties have some amount of variation stemming from the variation in modal parameters, thus, reliability of identified modal parameters directly affects the reliability of extracted properties of structural elements and so condition assessment of the structure.

4. EFFECT OF TRAFFIC LOADING

4.1. General

There have been many studies [27-29, 47-50] concerning the vehicle-bridge interaction. Within those studies, change in the dynamic behavior of bridges such as modal frequencies, dynamic amplification factor, static and dynamic deflections have been investigated. Many vehicle-bridge interaction elements have been developed for finite element model analyses. The main factors with significant influences on the dynamic behavior of a bridge could be stated as follows:

- Vehicle mass
- Vehicle speed and acceleration
- Vehicle suspension characteristics (matching of bridge and vehicle natural frequencies)
- Roughness of the interaction surface

In this section, by using finite element models presented in Chapter 3, effects of static mass, correlated input and speed parameter of moving loads are presented as the primary reasons for the variation in identified modal frequencies of bridges.

4.2. Static Mass Analyses

Mass and stiffness parameters of structural elements are the main components that have significant influences on modal parameters. Changes in modal frequencies are expected due to the additional mass accounting for the bridge deck.

In order to represent three typical vehicles, three different mass quantities were defined for this analysis:

- 2 tons mass: Passenger Car / Sport Utility Vehicle (PC/SUV)

- 18.13 tons mass: A mid size truck (H20 Truck)
- 32.63 tons mass: A big size truck (HS20 Truck)

These masses are applied to the bridge model as lumped masses to the nodes. The nodes are shown in the Figure 4.1.

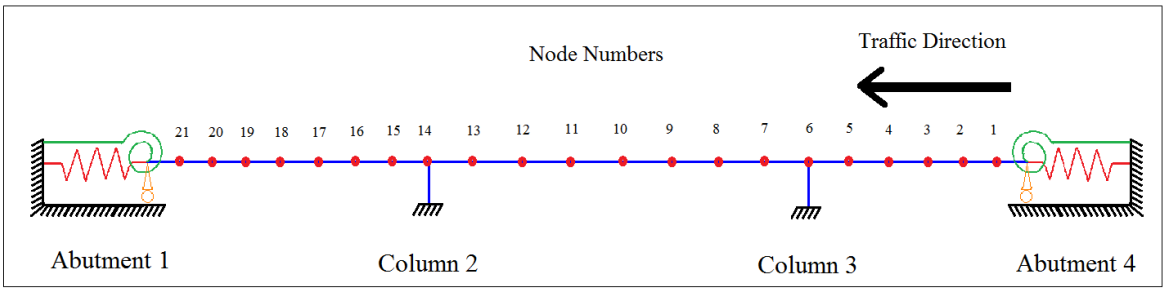

Figure 4.1. Node numbers for the static mass analysis.

In the first part, masses are applied at only one node of the bridge. Results are given in Table 4.1 for the single lumped mass analysis. Increase in mass results in decrease in modal frequencies as it was expected. The amount of change depends on the node number of the additional mass. Shifting the location of the mass, the distribution for the modal mass of lumped mass was changed for different modes. Maximum amount of changes for each mode were investigated within different nodes. Maximum change in the first natural frequency was observed as -4.5% when the mass of HS210 Truck was added to the midpoint of the second span. Over all maximum change occurred in fourth natural frequency as -5.1%.

In the second part of this analysis, masses are applied at two different nodes at the same time. Distance between two lumped masses is selected as approximately 45 meters which represents the safe following distance for moving vehicles in highways. Results are given in Table 4.2 for double lumped mass analysis.

Maximum change in the first natural frequency was observed as -4.8% with the effect of two masses of HS21 Truck. Although the total amount of lumped masses is two times bigger than previous analysis, differences between the changes in the first natural

frequencies of these two analyses are too close. Over all maximum change has occurred in second natural frequency as -5.5%.

All in all, additional masses have significant effects on the distribution of the modal mass of the system. Change in this distribution is the main factor affecting the amount of the changes in natural frequencies. Numbers, locations and mass of the vehicles are very critical for instant modal frequencies of the bridge.

Table 4.1. Changes in the modal frequencies of the single lumped mass analysis.

Node Number	Change in natural frequencies (%)														
	PC/SUV					H20 Truck					HS20 Truck				
	1st	2nd	3rd	4th	5th	1st	2nd	3rd	4th	5th	1st	2nd	3rd	4th	5th
1	0.0	0.0	-0.1	-0.1	0.0	0.0	-0.1	-0.5	-1.0	-0.2	0.0	-0.1	-1.0	-1.8	-0.3
2	0.0	0.0	-0.1	-0.3	0.0	0.0	-0.2	-1.2	-2.7	-0.3	-0.1	-0.3	-2.2	-4.6	-0.6
3	0.0	0.0	-0.1	-0.4	0.0	-0.1	-0.2	-1.5	-3.0	-0.3	-0.1	-0.5	-2.8	-5.1	-0.5
4	0.0	0.0	-0.1	-0.2	0.0	-0.1	-0.2	-1.1	-1.8	-0.1	-0.1	-0.4	-2.0	-3.2	-0.2
5	0.0	0.0	-0.1	0.0	0.0	0.0	-0.1	-0.5	-0.5	0.0	0.0	-0.2	-0.9	-0.9	-0.1
6	0.0	0.0	0.0	0.0	-0.1	-0.2	-0.2	-0.4	-0.2	-0.7	-0.3	-0.3	-0.7	-0.3	-1.3
7	-0.1	0.0	0.0	0.0	-0.3	-1.0	-0.4	-0.3	-0.2	-2.4	-1.7	-0.8	-0.6	-0.3	-4.1
8	-0.2	0.0	0.0	0.0	-0.2	-2.0	-0.5	-0.3	-0.2	-1.6	-3.6	-0.9	-0.5	-0.3	-2.7
9	-0.3	0.0	0.0	0.0	0.0	-2.5	-0.3	-0.4	-0.3	0.0	-4.5	-0.6	-0.7	-0.4	-0.1
10	-0.2	0.0	-0.1	0.0	-0.2	-2.2	-0.1	-0.6	-0.3	-1.3	-3.8	-0.2	-1.0	-0.5	-2.3
11	-0.1	0.0	-0.1	0.0	-0.3	-1.1	0.0	-0.6	-0.2	-2.4	-2.0	-0.1	-1.0	-0.4	-4.1
12	0.0	0.0	0.0	0.0	-0.1	-0.2	-0.1	-0.3	-0.2	-0.9	-0.5	-0.1	-0.6	-0.3	-1.6
13	0.0	0.0	0.0	0.0	0.0	-0.1	-0.2	-0.3	-0.2	-0.1	-0.1	-0.4	-0.5	-0.3	-0.1
14	0.0	-0.1	0.0	0.0	0.0	-0.2	-1.0	-0.3	-0.2	-0.1	-0.5	-1.8	-0.6	-0.3	-0.1
15	0.0	-0.2	-0.1	0.0	0.0	-0.4	-2.0	-0.5	-0.2	0.0	-0.8	-3.5	-0.9	-0.3	-0.1
16	0.0	-0.3	-0.1	0.0	0.0	-0.5	-2.7	-0.8	-0.2	-0.1	-0.9	-4.7	-1.4	-0.4	-0.1
17	0.0	-0.3	-0.1	0.0	0.0	-0.4	-2.5	-0.9	-0.2	-0.2	-0.7	-4.4	-1.6	-0.4	-0.3
18	0.0	-0.1	-0.1	0.0	0.0	-0.2	-1.6	-0.7	-0.2	-0.2	-0.4	-2.8	-1.3	-0.4	-0.3
19	0.0	0.0	0.0	0.0	0.0	0.0	-0.4	-0.4	-0.2	-0.1	-0.1	-0.8	-0.7	-0.4	-0.1
20	0.0	0.0	0.0	0.0	0.0	0.0	0.0	-0.3	-0.1	0.0	0.0	-0.1	-0.5	-0.2	-0.1
21	0.0	0.0	0.0	0.0	0.0	0.0	0.0	-0.2	-0.2	0.0	0.0	-0.1	-0.4	-0.3	0.0
MAX	-0.3	-0.3	-0.1	-0.4	-0.3	-2.5	-2.7	-1.5	-3.0	-2.4	-4.5	-4.7	-2.8	-5.1	-4.1

Table 4.2. Changes in the modal frequencies of the double lumped mass analysis.

Node Number	Change in natural frequencies (%)														
	PC/SUV					H20 Truck					HS20 Truck				
	1st	2nd	3rd	4th	5th	1st	2nd	3rd	4th	5th	1st	2nd	3rd	4th	5th
1-11	-0.2	0.0	-0.1	-0.1	-0.2	-2.2	-0.2	-1.1	-1.3	-1.5	-3.8	-0.4	-2.0	-2.3	-2.6
2-12	-0.1	0.0	-0.2	-0.3	-0.3	-1.2	-0.2	-1.7	-2.9	-2.7	-2.1	-0.4	-3.1	-5.0	-4.7
3-13	0.0	0.0	-0.2	-0.4	-0.1	-0.3	-0.3	-1.8	-3.2	-1.2	-0.6	-0.6	-3.2	-5.4	-2.0
4-14	0.0	0.0	-0.1	-0.2	0.0	-0.1	-0.2	-1.3	-2.0	-0.1	-0.1	-0.5	-2.3	-3.5	-0.2
5-15	0.1	0.0	-0.1	-0.1	0.0	-0.1	-0.3	-0.8	-0.7	-0.1	-0.2	-0.6	-1.3	-1.2	-0.2
6-16	0.0	-0.1	-0.1	0.0	0.0	-0.2	-1.0	-0.6	-0.4	-0.1	-0.4	-1.8	-1.0	-0.5	-0.2
7-17	0.0	-0.2	-0.1	0.0	-0.1	-0.6	-2.2	-0.9	-0.4	-0.8	-1.1	-3.8	-1.6	-0.6	-1.3
8-18	-0.1	-0.3	-0.1	0.0	-0.3	-1.4	-3.2	-1.2	-0.4	-2.4	-2.5	-5.5	-2.0	-0.6	-4.1
9-19	-0.2	-0.3	-0.1	0.0	-0.2	-2.3	-3.1	-1.2	-0.4	-1.7	-4.1	-5.4	-2.1	-0.7	-2.9
10-20	-0.3	-0.2	-0.1	0.0	0.0	-2.7	-2.0	-1.1	-0.5	-0.2	-4.8	-3.5	-2.0	-0.8	-0.4
11-21	-0.2	0.0	-0.1	0.0	-0.2	-2.2	-1.4	-1.0	-0.5	-1.4	-3.9	-1.1	-1.7	-0.9	-2.4
MAX	-0.3	-0.3	-0.2	-0.4	-0.3	-2.7	-3.2	-1.8	-3.2	-2.7	-4.8	-5.5	-3.2	-5.4	-4.7

4.3. Moving Load Analysis of Single Span Beams

4.3.1. Analytical Solution of Moving Load Problem

In this part an analytical solution of moving load problem is represented. A simply supported beam subjected to a moving load is shown in Figure 4.2. Modulus of elasticity, moment of inertia and unit mass of the beam are constant over the length.

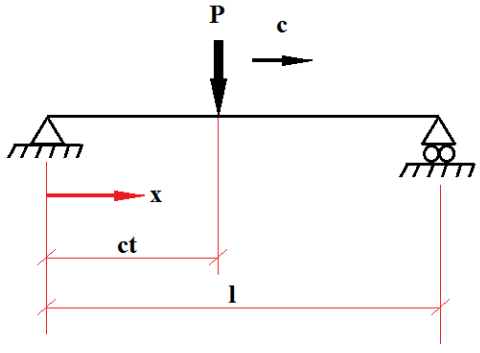

Figure 4.2. A moving load model.

The weight of the passing vehicle is represented by a concentrated constant point load and the inertial effect of the load is not considered. This point load is travelling on the beam at a constant speed.

The governing equation of motion of a simply supported elastic beam under the effect of a moving load can be described by Bernoulli-Euler's differential equation as:

$$EI\frac{\partial^4(v(x,t))}{\partial x^4} + m\frac{\partial^2(v(x,t))}{\partial t^2} + 2m\omega_b\frac{\partial(v(x,t))}{\partial t} = \delta(x-ct)P \qquad (4.1)$$

where E is the modulus of elasticity, I is the moment of inertia, $v(x,t)$ is deflection at point x and time t, ω_b is the circular frequency of damping, m is the unit mass of the beam, P is constant point load and c is constant speed of the point load.

Boundary conditions for this problem are:

$$v(0,t) = 0\ ;\ v(l,t) = 0\ ;\ \frac{\partial^2(v(x,t))}{\partial x^2}\Big|_{x=0} = 0\ ;\ \frac{\partial^2(v(x,t))}{\partial x^2}\Big|_{x=l} = 0 \qquad (4.2)$$

and initial conditions can be defined as:

$$v(x,0) = 0\ ;\ \frac{\partial(v(x,t))}{\partial t}\Big|_{t=0} = 0 \qquad (4.3)$$

Equation 4.1 can be solved by the method of Fourier sine integral transformation considering the initial and boundary conditions given in Equation 4.2 and Equation 4.3, respectively [51]. The transformation of the deflection of the beam is described as:

$$V(j,t) = \int_0^l v(x,t)\,sin\frac{j\pi x}{l}\,dx, \qquad j = 1,2,3,\ldots$$

$$v(x,t) = \frac{2}{l}\sum_{j=1}^{\infty} V(j,t)\,sin\frac{j\pi x}{l} \qquad (4.4)$$

where $V(j,t)$ is the *j*th normal mode vibration of this beam.

By using the Fourier sine integral transformation Equation 4.1 become a continuous time equation of motion for the *j*th mode of the generalized deflection as:

$$\frac{d^2(V(j,t))}{dt^2} + 2\omega_b \frac{d(V(j,t))}{dt} + \omega_{(j)}^2 V(j,t) = \frac{P}{m} sin\, j\omega t \tag{4.5}$$

where $\omega_{(j)}$ is the natural frequency of *j*th mode:

$$\omega_{(j)} = \frac{j^2\pi^2}{l^2}\left(\frac{EI}{m}\right)^{\frac{1}{2}} \tag{4.6}$$

and ω is the circular frequncy:

$$\omega = \frac{\pi c}{l} \tag{4.7}$$

Final form of the solution of Equation 3.1 was given [51] as:

$$\begin{aligned} v(x,t) = \left(\frac{2Pl^3}{\pi^4 EI}\right)\sum_{j=1}^{\infty} \frac{1}{j^2[j^2(j^2-\alpha^2)^2 + 4\alpha^2\alpha^2]}\Bigg[& j^2(j^2-\alpha^2)\, sin\, j\omega t \\ & - \frac{j\alpha[j^2(j^2-\alpha^2) - 2\alpha^2]}{(j^4-\beta^2)^{1/2}} e^{-\omega_b t}\, sin\, \omega'_{(j)} t \\ & - 2j\alpha\beta\left(cos\, j\omega t - e^{-\omega_b t}\, cos\, \omega'_{(j)} t\right)\Bigg] sin\frac{j\pi x}{l} \end{aligned} \tag{4.8}$$

where α is a dimensionless speed parameter:

$$\alpha = \frac{\omega}{\omega_{(1)}} = \frac{c}{c_{cr}} \tag{4.9}$$

β is a dimensionless damping parameter:

$$\beta = \frac{\omega_b}{\omega_{(1)}} \tag{4.10}$$

and $\omega'_{(j)}$ is the circular frequency of lightly damped beam:

$$\omega'_{(j)} = \left(\omega^2_{(j)} - \omega^2_b\right)^{1/2} \tag{4.11}$$

This solution is only valid for $0 \leq t \leq l/c$. When the moving load leaves the bridge, for $t > l/c$, the motion of the beam becomes free vibration. Although the problems solved by the assumption of constant natural frequencies, irrelevant to speed, in Equation 4.6, deflections are quite related to the speed. Speed related deflections, then, cause variations, as shown in the following parts.

4.3.2. Correlated White Noise Analysis of a Single Span Beam

A single span beam model is created to represent the effect of correlated white noise in identified modal parameters, seen in Figure 4.3. Beam is supported at vertical and rotational springs to represent abutment conditions. It has constant modulus of elasticity, moment of inertia and unit mass values over the length. Properties of this FEM are given in Table 4.3. Natural frequencies of the first two modes are converged at 3.40 and 9.35 Hz, respectively, in FEM with 60 elements.

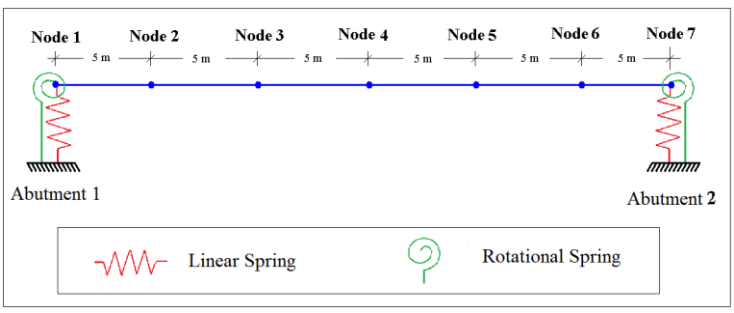

Figure 4.3. FEM for correlated white noise analysis.

Table 4.3. Properties of the structural elements and boundary conditions of FEM.

Properties		Beam	Abutments
Crossectional Area	(m^2)	6.0	N/A
Moment of inertia	(m^2)	0.5	N/A
Modulus of elasticity	(MPa)	25000	N/A
Unit mass	(kg/m^3)	2400	N/A
Total length	(m)	30	N/A
Longitudinal spring stiffness	(N/m)	N/A	$2.0\ 10^{11}$
Rotational spring stiffness	(N.m/rad)	N/A	$2.0\ 10^{10}$

A Gaussian white noise is created as an input source and shown in Figure 4.4. It does not contain dominant frequencies up to 50 Hz that this white noise satisfies our conditions. PSD of the created white noise is shown in Figure 4.5.

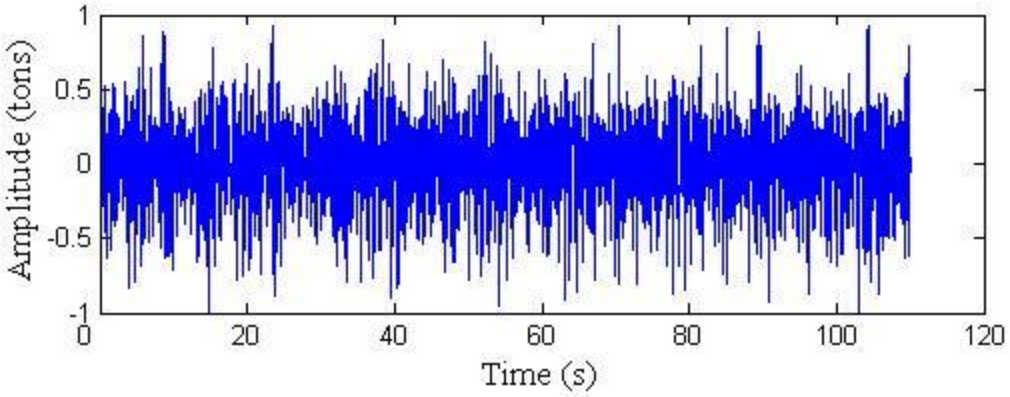

Figure 4.4. White noise input.

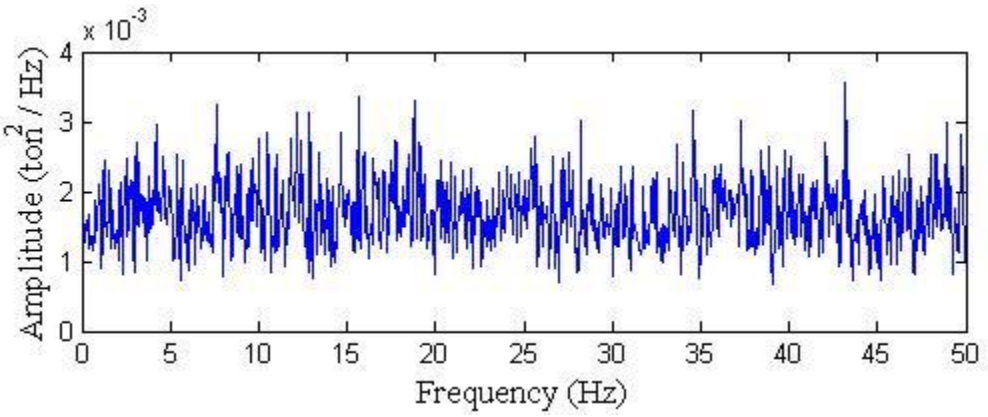

Figure 4.5. PSD of the white noise input.

This white noise is applied to the adjacent input nodes within a time delay. This time delay represents the speed of moving environment across the beam. Five different cases are considered, with different time delays, in this analysis. Properties and results of these case analyses are given in Table 4.4.

Table 4.4. Case analyses and results.

Case Analyses	Speed Calculation			Results	
	Distance between two adjacent input nodes	Delay between two nodes	Associated vehicle speed	First modal frequency	Second modal frequency
	(m)	(s)	(m/s)	(Hz)	(Hz)
Case 1	5	0.600	8.33	3.37	8.69-9.81
Case 2	5	0.400	12.50	4.35	9.13
Case 3	5	0.225	22.22	3.37	9.13
Case 4	5	0.150	33.33	3.37	9.81
Case 5	5	0.100	50.00	N/A	9.13

A typical acceleration output of the fourth node is given in Figure 4.6. Acceleration output data sets, considering all nodes, are analyzed by using FDD algorithm. Singular values of the PSD matrices for all cases are given in Figure 4.7. The red lines mark the first two natural frequencies of the beam model without any external excitations.

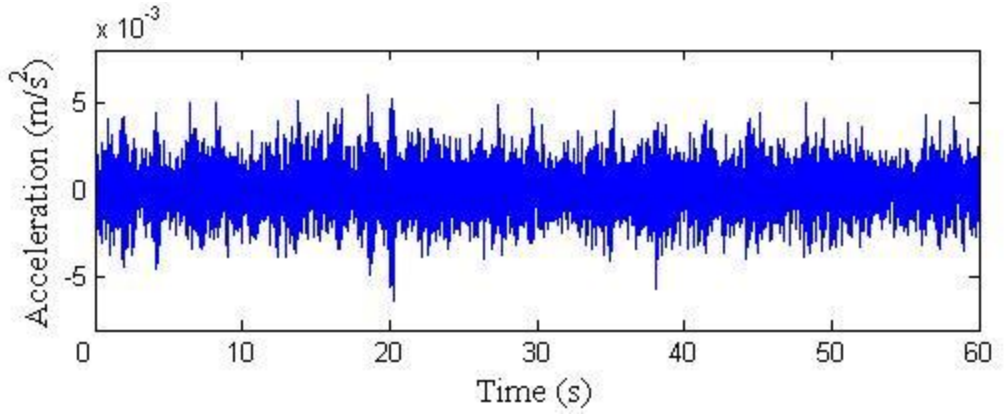

Figure 4.6. A typical acceleration output of the node 4.

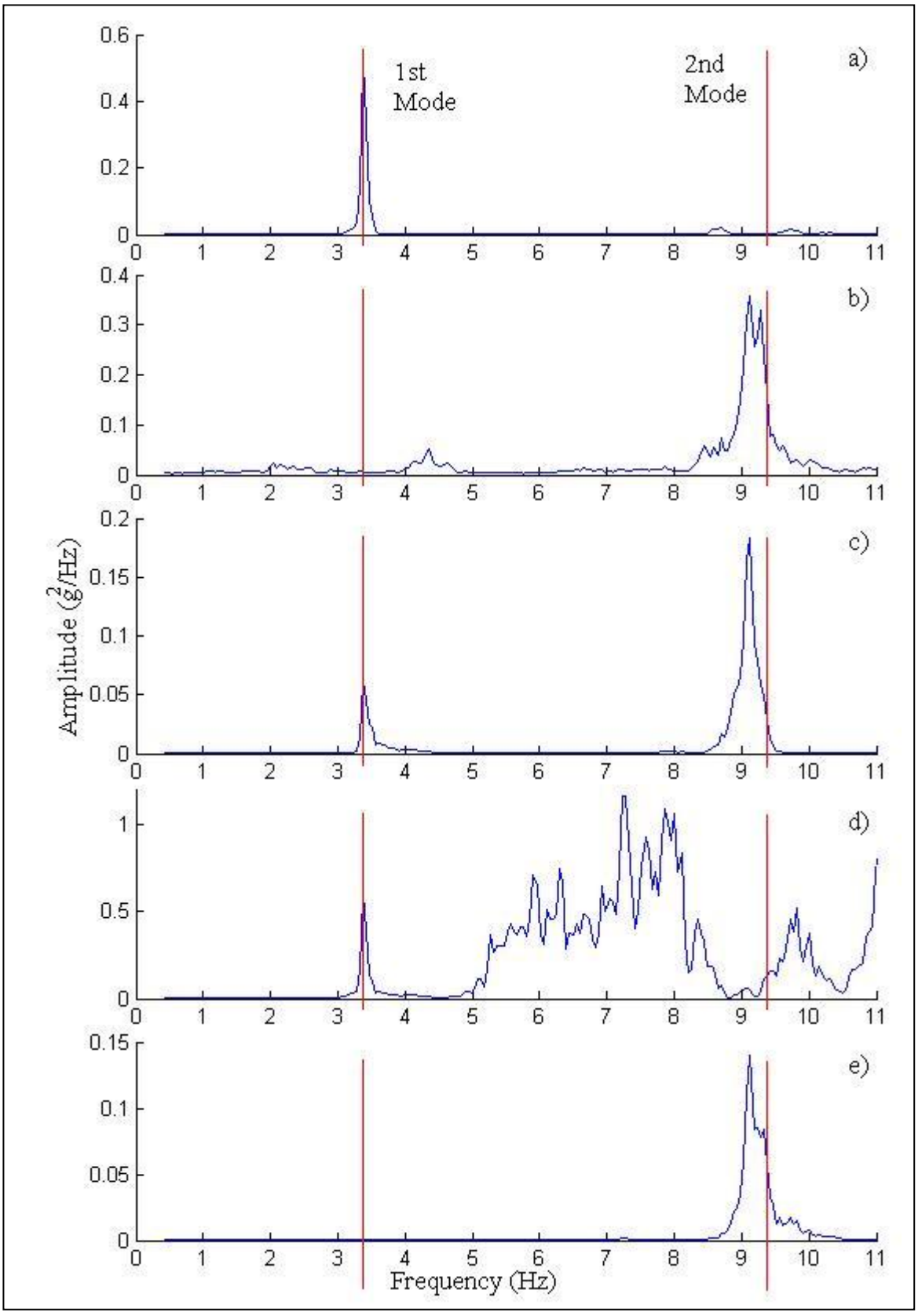

Figure 4.7. Singular values of PSD matrices for (a) Case 1 (b) Case 2 (c) Case 3 (d) Case 4 (e) Case 5.

In Case 2 and 5, the first mode of vibration is suppressed. However, a non-negligible misleading peak occurs at frequency of 4.27 Hz for the Case 2. More importantly, in Case 1 the second mode is also suppressed while two pseudo peaks appear around the second frequency. In Case 4, many pseudo peaks are observed between first two modal frequencies, and second frequency is found at 9.66 Hz.

When neglecting the complicated vehicle-bridge interaction effects, traffic excitation automatically becomes correlated. Input of the vehicle acts on all nodes with the same manner with a time delay related to its speed. This correlation leads to misleading results in identified modal parameters as indicated in the moving load and correlated white noise analyses.

4.4. FEM Analysis of Moving Load Problem of the JRO

In this part, Finite Element Model (FEM) analyses for the moving load problem are represented. A FEM of the JRO created according to the design drawings is represented in Chapter 3. Different moving load analyses are conducted with different load cases. Figure 4.8 shows the effect of moving load during the analysis.

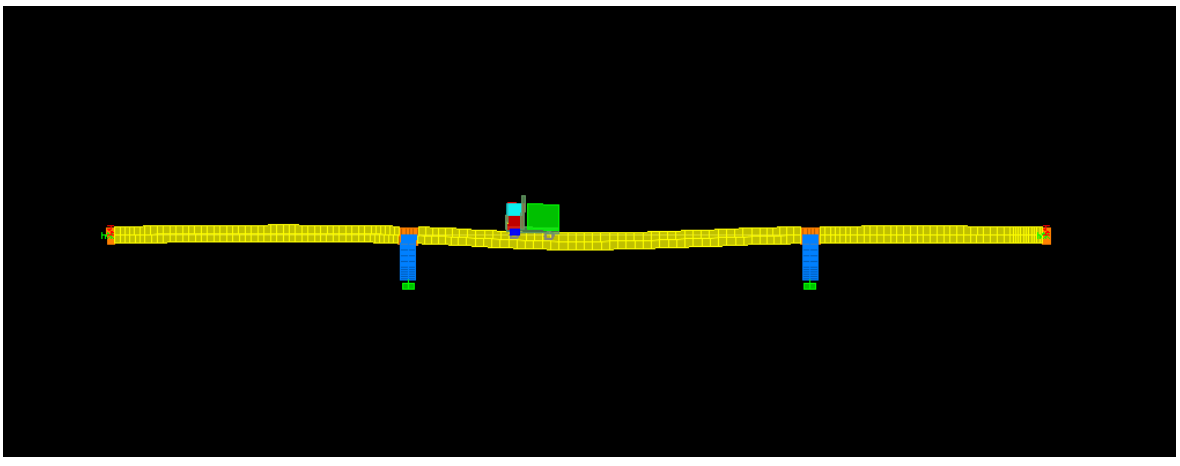

Figure 4.8. FEM of the moving load.

Five different vehicle models are defined for moving load analyses which are:

- Type 1: 1-Point load model to roughly represent all types of vehicles.

- Type 2: 2-Point load model with 2.6 m wheelbase and equal axle loads to represent passenger cars.
- Type 3: 2-Point load model with 4.3 m wheelbase and equal axle loads to represent medium duty trucks.
- Type 4: 2-Point load model with 4.3 m wheelbase with different axle loads to represent heavy duty trucks.
- Type 5: 3-Point load model with 2.6 m wheelbase with equal axle loads to represent a 3-axle imaginary vehicle.

These vehicle models are analyzed in FEM with 10 different speeds from 15 km/h to 150 km/h with an increment of 15km/h. Acceleration data from five different nodes, as close as possible to the acceleration sensors instrumented at the JRO, is used in the identification process. Fifty data sets are analyzed in total and first modal frequencies are identified by using FDD algorithm. Singular values of PSD matrices for analyses are plotted in Figure 4.9-13.

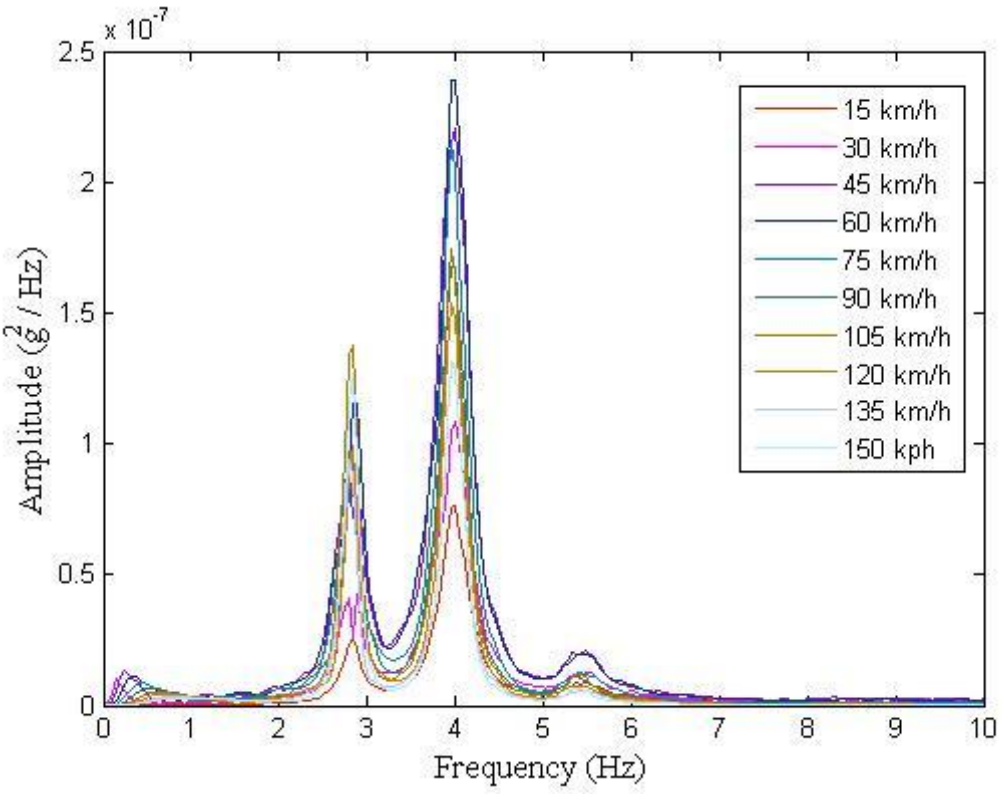

Figure 4.9. Singular values of PSD matrices for Type 1 analyses.

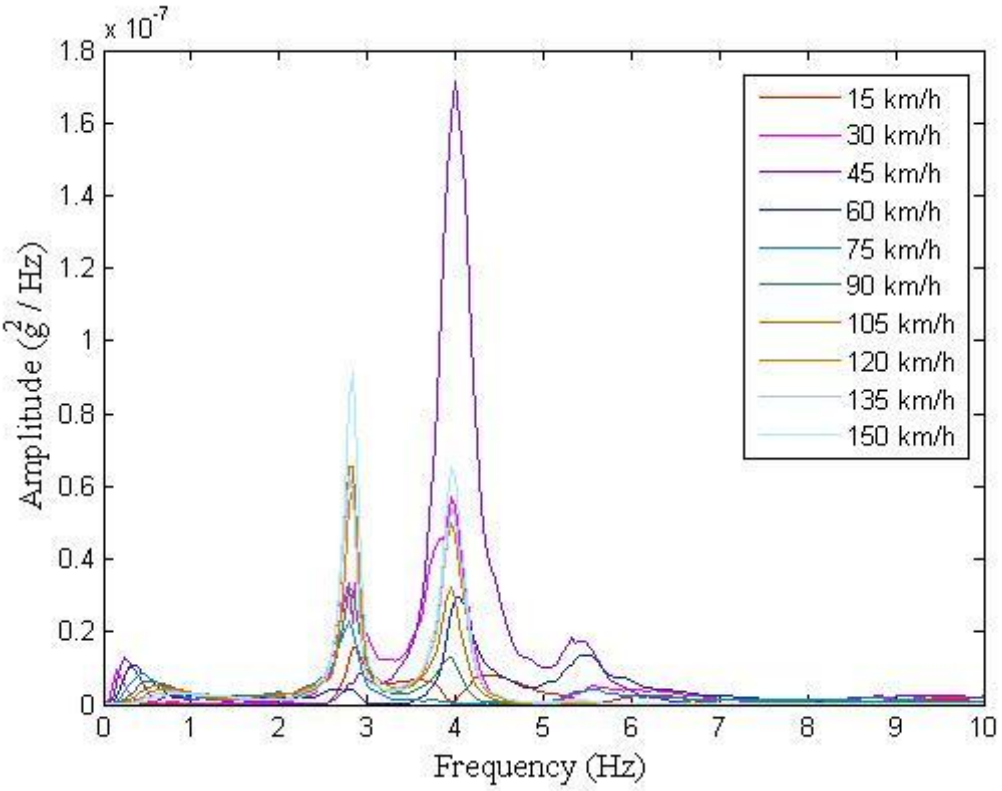

Figure 4.10. Singular values of PSD matrices for Type 2 analyses.

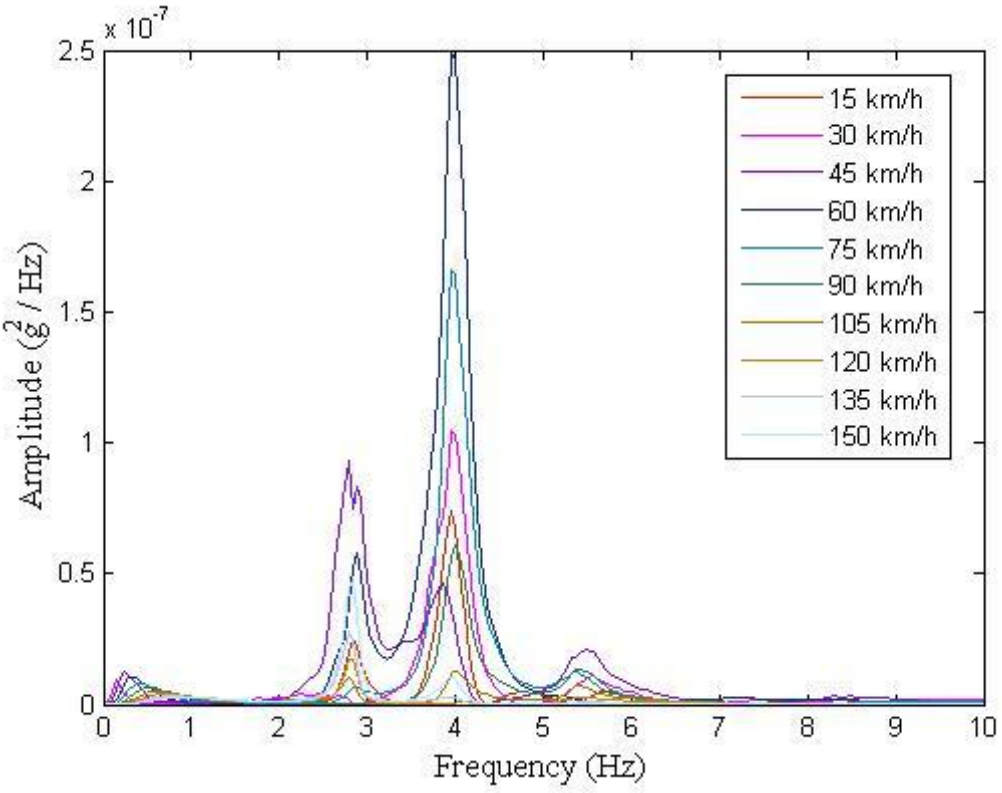

Figure 4.11. Singular values of PSD matrices for Type 3 analyses.

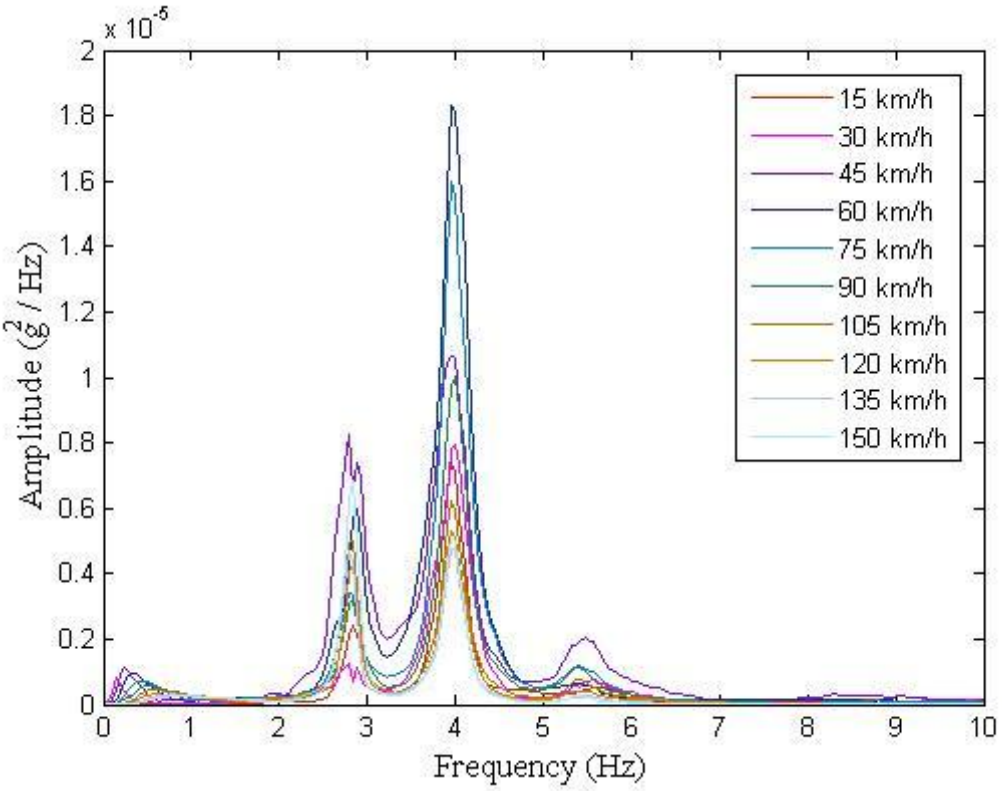

Figure 4.12. Singular values of PSD matrices for Type 4 analyses.

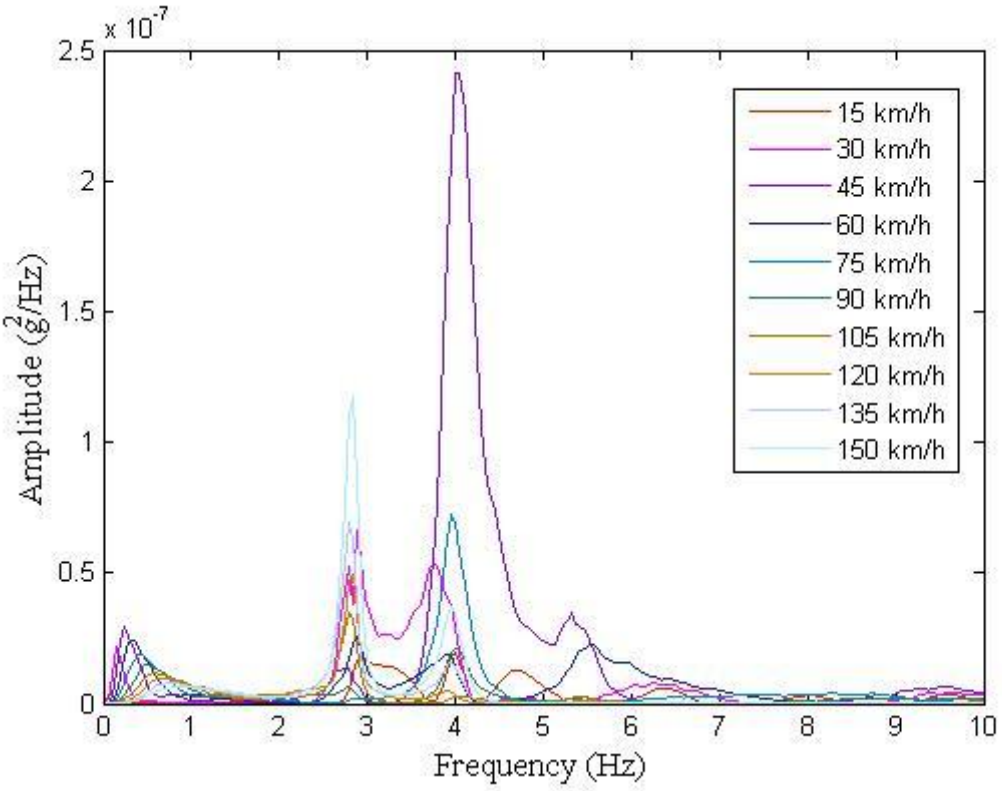

Figure 4.13. Singular values of PSD matrices for Type 5 analyses.

The identified modal parameters are shown in Figure 4.14. The red lines mark the first natural frequency of the bridge without any external excitations.

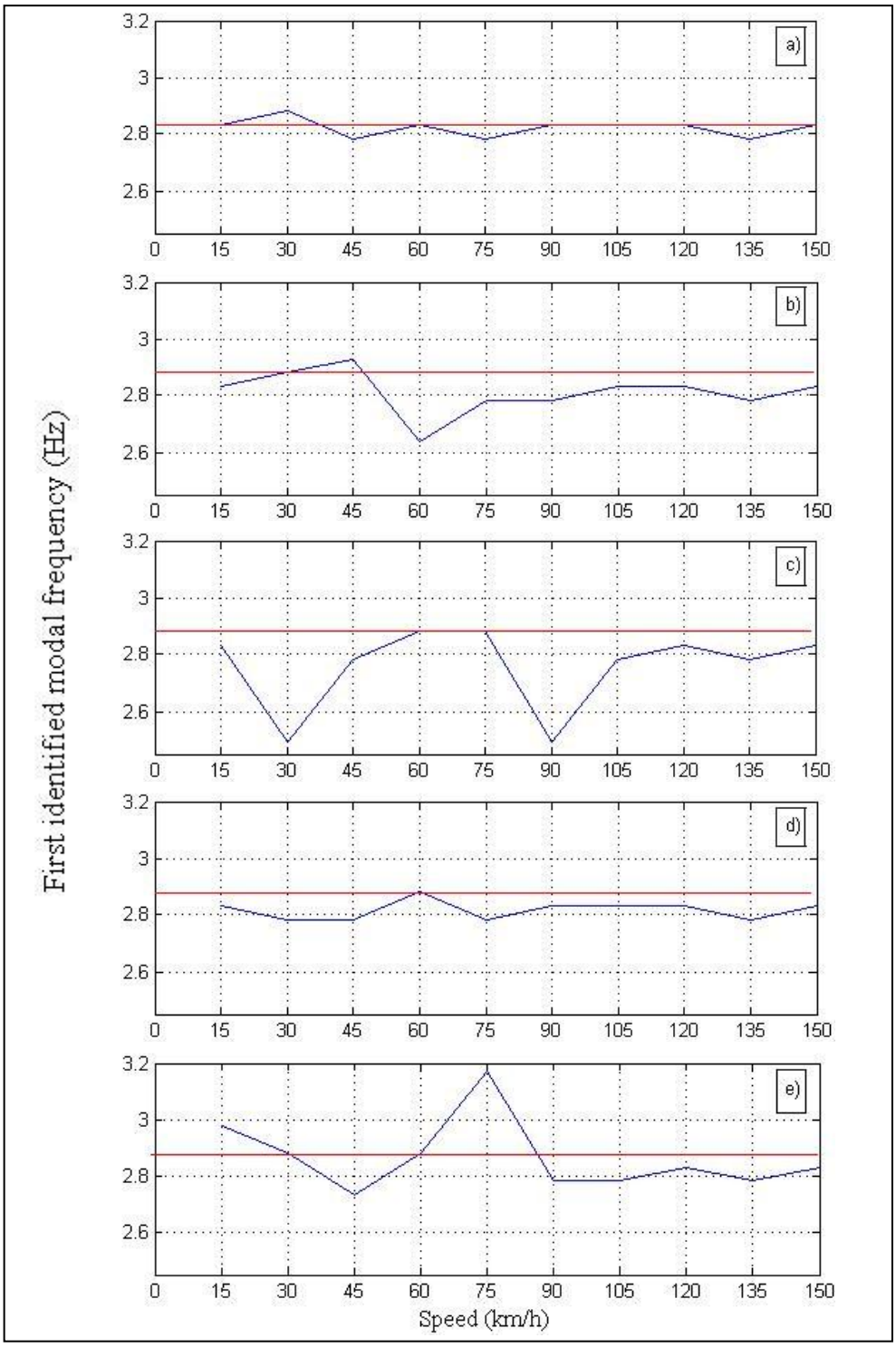

Figure 4.14. Identified first modal frequencies from moving load analyses for (a) Type 1 (b) Type 2 (c) Type 3 (d) Type 4 (e) Type 5.

Changes in identified modal frequencies are observed as the vehicle speed changes; however, these changes vary for different types of vehicle models. Consequently, the change in identified modal frequencies cannot be described by only speed or vehicle model. Different combinations of these parameters result in different change patterns.

A sample analysis result of a well identified data set (Type 4 with 150 km/h) is given in Figure 4.15. Almost all modes are clearly identified from this data set.

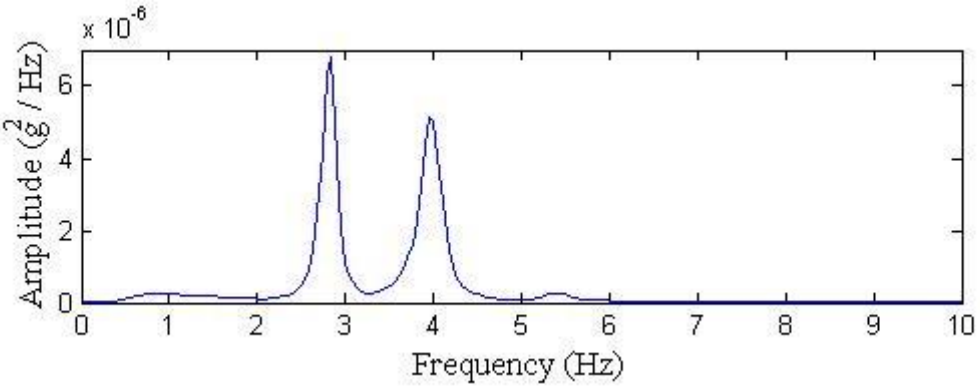

Figure 4.15. Singular values of PSD matrice for Type 4 analysis with 150 km/h speed.

However, in some other cases, changes in identified modal parameters are observed. Figure 4.16 and Figure 4.17 demonstrate these changes in the first modal frequencies. These changes are observed from the data sets of Type 3 with 30 km/h and Type 2 with 60 km/h, respectively.

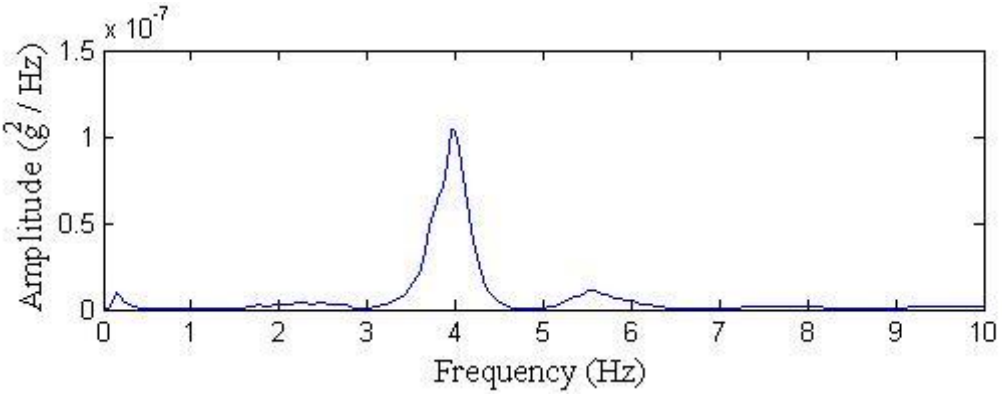

Figure 4.16. Singular values of PSD matrice for Type 3 analysis with 30 km/h speed.

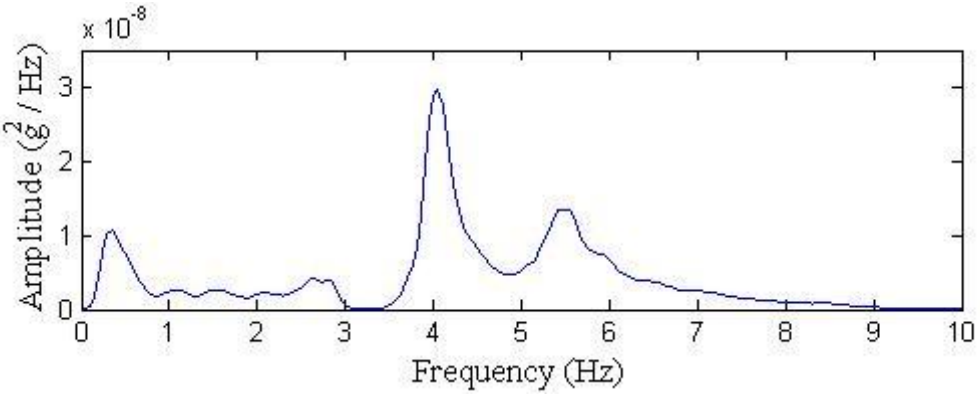

Figure 4.17. Singular values of PSD matrice for Type 2 analysis with 60 km/h speed.

As observed from the results of the data sets of Type 3 with 90 km/h and Type 5 with 75 km/h, first modal frequency cannot be identified due to the insufficient excitation of different modes including the first mode. Figure 4.18 and Figure 4.19 demonstrate this problem.

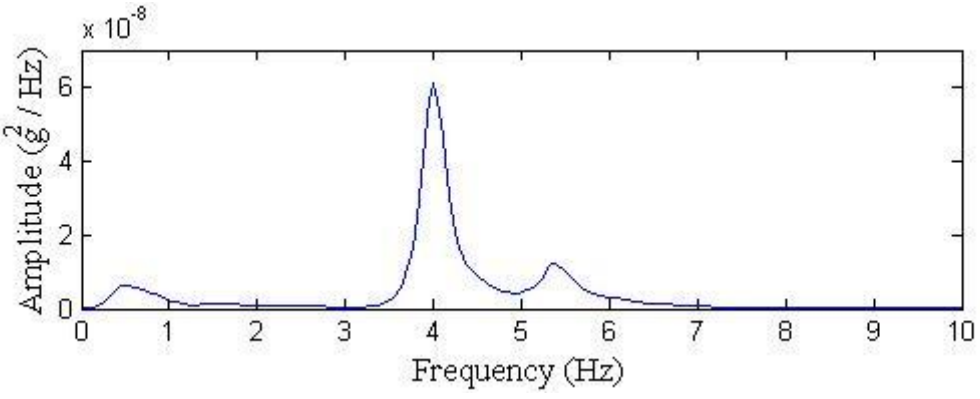

Figure 4.18. Singular values of PSD matrice for Type 3 analysis with 90 km/h speed.

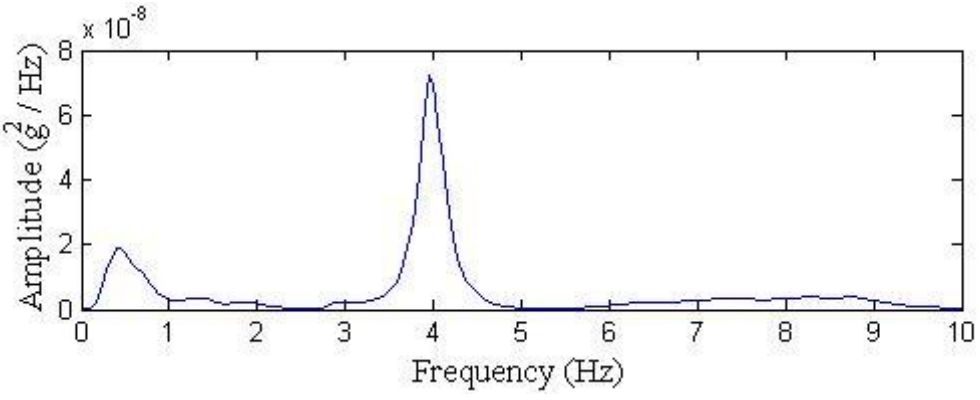

Figure 4.19. Singular values of PSD matrice for Type 5 analysis with 75 km/h speed.

The effect of speed on the dynamic amplification factor was demonstrated by Awall *et al*. [28]. Four different bridge models having different radius of horizontal curvature values were analyzed with the same vehicle model with four different speeds. Figure 4.20 shows the change in dynamic characteristics with the change in speed.

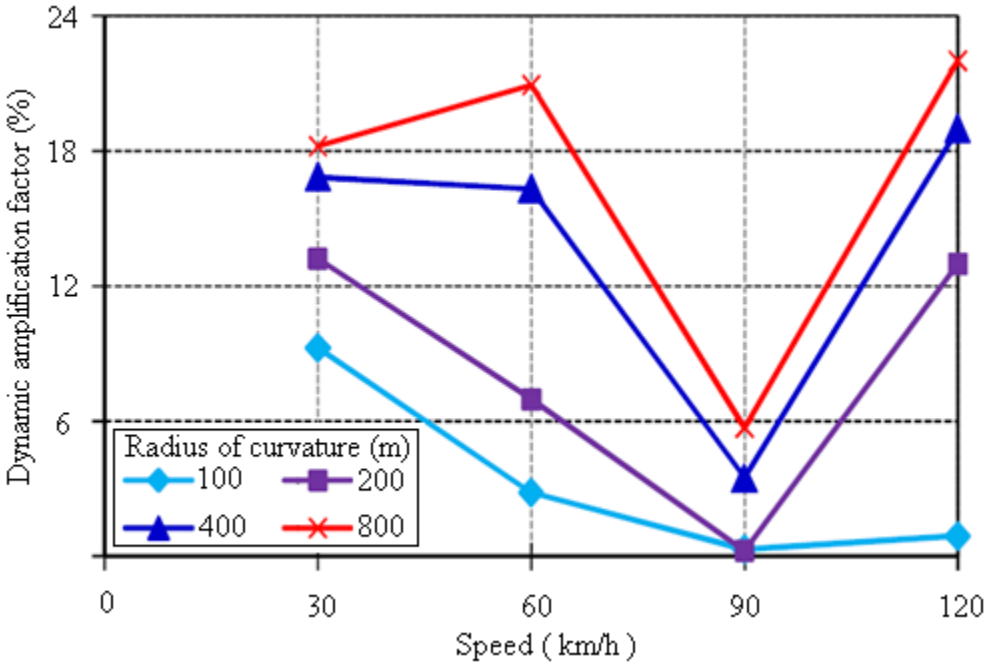

Figure 4.20. Effect of the speed on dynamic amplification factor [28].

In this thesis, effect of speed on the identified modal parameters is also demonstrated. Although the speed of moving loads has a significant influence on the change in modal frequencies, this effect is not always the same for different types of vehicle models. Consequently, wheelbase of the vehicle models becomes a complementary factor in the effect of speed parameter.

4.5. Discussion in Cross-Correlation and Speed

Within the study, it is also aimed to determine the speed of the vehicles from measurements in order to observe the relation with the identified modal parameters. The first ways is visually selecting two correlated peaks in different vertical acceleration sensors. The second way, gives more accurate results, is to use cross-correlation function for time delay between two nodes.

Then, the speed of the vehicle can be calculated by dividing the distance between the sensor locations by the time delay between corresponding peaks. An acceleration data including well separated acceleration peaks is shown in the Figure 4.21. For example, distance between these two channels is 79 meters. The time delay for the second peak is 3.47 seconds. With these values speed of the second vehicle is calculated as 82 km/h.

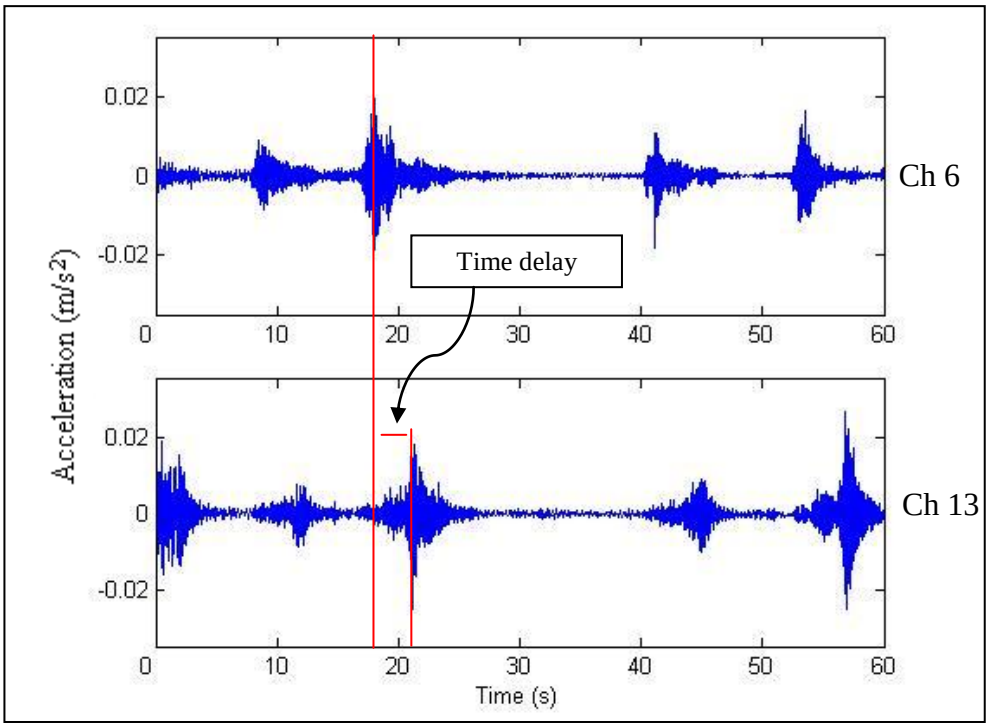

Figure 4.21. Well separated acceleration peaks for time delay calculation.

Both methods result in acceptable results when responses are due to the same vehicle without any disturbance of other vehicles are used; however, in many acceleration data, disturbances of different vehicles are visually observed as seen in the Figure 4.22. This situation results in misleading time delays.

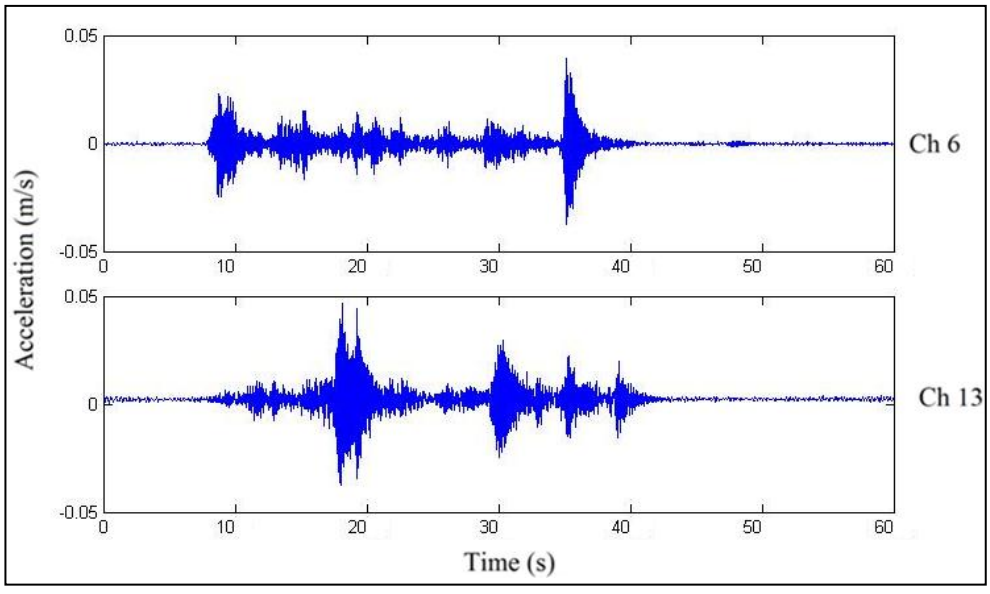

Figure 4.22. Disturbances of the different vehicles.

5. CONCLUSIONS AND RECOMMENDATIONS

5.1. Conclusions

This thesis presents the effect of traffic loading on the variations in modal parameters of bridges. First of all, variations are presented by analyzing traffic-induced vibration measurements of the JRO. Variations up to 10% in identified modal frequencies and 6% in structural properties are observed. To investigate the effects of traffic loading on the variations, three finite element analyses are carried out which are static mass, correlated white noise and moving load analyses. From the results of these analyses, the following observations can be made:

- Additional masses have significant contributions in modal mass of the system. Change in the modal mass is the main factor affecting the amount of changes in natural frequencies for static case. Numbers, locations and quantities of the additional masses are the determinative factors of the decrease in modal frequencies.
- The same white noise is applied to the consecutive nodes of a beam model within a time delay to make the inputs correlated. By changing the delay values, five different cases are analyzed. These correlated white noise analyses result in suppressed modes, pseudo peaks and shifts in identified natural frequencies.
- Speed of the moving loads has significant effects on the natural frequencies of bridges. In addition, wheelbase properties of the moving vehicle models, used as moving loads, cause different responses for the same speeds.

5.2. Recommendations

Recommendations for further studies can be listed as follows:

- In the moving load analysis, only one moving vehicle model passes through the bridge per each case. To obtain accurate results of moving load analysis, it would be better to use more sophisticated vehicle-bridge interaction models including inertial

effects of loads, suspension models of vehicles, roughness of the interaction surface and accelerating speed. Different combinations of different moving vehicle models with different numbers and speeds can be used for extended studies.

- Correlated white noise analysis is conducted with limited number of input nodes. Distance between two consecutive nodes for inputs is taken as six meters. Increasing the number of input nodes might give more accurate results.

REFERENCES

1. Farrar, C. R. and K. Worden, "An Introduction to Structural Health Monitoring", *Philosophical Transactions Royal Society A: Mathematical, Physical and Engineering Sciences*, Vol. 365, No. 1851, pp. 303-315, 2007.

2. Federal Highway Administration, *Code of Federal Regulations for the National Bridge Inspection Standards*, U.S. Government Printing Office, 23CFR650, 1996.

3. Federal Highway Administration, *Recording and Coding Guide for the Structure Inventory and Appraisal of the Nation's Bridges*, U.S. Department of Transportation, FHWA-PD-96-001, 1995.

4. Phares, B. M., G. A. Washer, D. D. Rolander, B. A. Graybeal and M. Moore, "Routine Highway Bridge Inspection Condition Documentation Accuracy and Reliability", *Journal of Bridge Engineering*, Vol. 9, No. 4, pp. 403–413, 2004.

5. Federal Highway Administration, *The Long-Term Bridge Performance Program*, 2008, http://www.fhwa.dot.gov/research/tfhrc/programs/infrastructure/structures/ltbp/, accessed at July 2012.

6. Safak, E., "Adaptive Modeling, Identification and Control of Dynamic Structural Systems. I: Theory", *Journal of Engineering Mechanics*, Vol. 115, No. 11, pp. 2386-2405, 1989.

7. Safak, E., "Identification of Linear Structures Using Discrete-Time Filters", *Journal of Structural Engineering*, Vol. 117, No. 10, pp. 3064-3085, 1991.

8. Ghanem, R. and M. Shinozuka, "Structural System Identification I: Theory", *Journal of Engineering Mechanics*, Vol. 121, No. 2, pp. 255-264, 1995.

9. Shinozuka, M. and R. Ghanem, "Structural System Identification II: Experimental Verification", *Journal of Engineering Mechanics*, Vol. 121, No. 2, pp. 265-273, 1995.

10. Lus H., R. Betti and R. W. Longman, "Identification of Linear Structural Systems Using Earthquake-Induced Vibration Data", *Earthquake Engineering and Structural Dynamics*, Vol. 28, No. 11, pp. 1449-1467, 1999.

11. Doebling, S. W., C. R. Farrar, M. B. Prime and D. W. Shevitz, *Damage Identification and Health Monitoring of Structural and Mechanical Systems from Changes in Their Vibration Characteristics: A Literature Review*, Los Alamos National Laboratory Report, LA-13070-MS, 1996.

12. Sohn H., C. R. Farrar, F. M. Hemez, D. D. Shunk, D. W. Stinemates, B. R. Nadler and J. J. Czarnecki, *A Review of Structural Health Monitoring Literature*, Los Alamos National Laboratory Report, LA-13976-MS, 2004.

13. Maia N. M. M. and J. M. M. Silva, "Modal Analysis Identification Techniques", *Philosophical Transactions of the Royal Society A: Mathematical, Physical and Engineering Sciences*, Vol. 359, No. 1778, pp. 29-40, 2001.

14. Brownjohn J. M. W., "Structural Health Monitoring of Civil Infrastructure", *Philosophical Transactions of the Royal Society A: Mathematical, Physical and Engineering Sciences*, Vol. 365, No. 1851, pp. 589-622, 2007.

15. Carden E. P. and P. Fanning, "Vibration-Based Condition Monitoring: A Review", *Structural Health Monitoring*, Vol. 3, No. 4, pp. 355-377, 2004.

16. Choi, S., S. Park, R. Bolton, N. Stubbs and C. Sikorsky, "Periodic Monitoring of Physical Property Changes in a Concrete Box-Girder Bridge", *Journal of Sound and Vibration*, Vol. 278, No. 1, pp. 365–381, 2004.

17. Feng, M. Q. and E. Y. Bahng, "Damage Assessment of Jacketed RC Columns Using Vibration Tests", *Journal of Structural Engineering*, Vol. 125, No. 3, pp. 265–271, 1999.

18. Guan, H., V. M. Karbhari and C. S. Sikorsky, "Web-Based Structural Health Monitoring of an FRP Composite Bridge", *Computer-Aided Civil and Infrastructure Engineering*, Vol. 21, No. 1, pp. 39-56, 2006.

19. Feng, M. Q. and J. M. Kim, "Identification of a Dynamic System Using Ambient Vibration Measurements", *Journal of Applied Mechanics*, Vol. 65, No. 2, pp. 1010–1023, 1998.

20. Feng, M. Q., D. K. Kim, J. H. Yi and Y. B. Chen, "Baseline Models for Bridge Performance Monitoring", *Journal of Engineering Mechanics*, Vol. 131, No. 5, pp. 562–569, 2003.

21. Feng, M. Q., Y. Fukuda, Y. Chen, S. Soyoz, and S. Lee, *Long-Term Structural Performance Monitoring of Bridges*, Technical Report of the California Department of Transportation, 2006-UCI-02, 2006.

22. Feng, M. Q. and D. K. Kim, *Long-Term Structural Performance Monitoring of Two Highway Bridges*, Technical Report of the California Department of Transportation, RTA59A0155, 2001.

23. Levin, R. I. and N. A. J. Lieven, "Dynamic Finite Element Model Updating Using Neural Networks", *Journal of Sound and Vibration*, Vol. 210, No. 5, pp. 593–607, 1992.

24. Calcada, R., A. Cunha and R. Delgado, "Analysis of Traffic-Induced Vibrations in a Cable-Stayed Bridge. Part II: Numerical Modeling and Stochastic Simulation", *Journal of Bridge Engineering*, Vol. 10, No. 4, pp. 386–397, 2005.

25. Peeters, B. and G. DeRoeck, “One-year Monitoring of the Z24-Bridge: Environmental Effects Versus Damage Events”, *Earthquake Engineering and Structural Dynamics*, Vol. 30, No. 2, pp. 149–171, 2001.

26. Sohn, H., M. Dzwonczyk, E. Straser, A. S. Kiremidjian, K. H. Law and T. Meng, “An Experimental Study of Temperature Effect on Modal Parameters of the Alamosa Canyon Bridge”, *Earthquake Engineering and Structural Dynamics*, Vol. 28, No. 8, pp. 879–897, 1999.

27. Green, M. F. and D. Cebon, “Dynamic Interaction between Heavy Vehicles and Highway Bridges", *Computers and Structures*, Vol. 62, No. 2, pp. 253–264, 1997.

28. Awall M. R., T. Hayashikawa, T. Matsumoto and X. He, “Parametric Study on Bridge-Vehicle Interaction Dynamics of Horizontally Curved Twin I-Girder Bridge”, *The 8th International Conference on Structural Dynamics*, Leuven, Belgium, 2011.

29. Yang, Y. B. and J. D. Yau, “Vehicle-Bridge Interaction Element for Dynamic Analysis”, *Journal of Structural Engineering*, Vol. 123, No. 11, pp. 1512–1518, 1997.

30. Soyoz, S. and M. Q. Feng, “Long-Term Monitoring and Identification of Bridge Structural Parameters”, *Computer-Aided Civil and Infrastructure Engineering*, Vol. 121, No. 2, pp. 265-273, 2009.

31. Maia N. M. M. and J. M. M. Silva, *Theoretical and Experimental Modal Analysis*, Research Studies Press LTD., Taunton, 1997.

32. Caicedo J. M., S. J. Dyke and E. A. Johnson, “Natural Excitation Technique and Eigensystem Realization Algorithm for Phase I of the IASC-ASCE Benchmark Problem: Simulated Data”, *Journal of Engineering Mechanics*, Vol.130, No. 1, pp. 49-60, 2004.

33. Shen F., M. Zheng, D. Feng and F. Xu, "Using the Cross-Correlation Technique to Extract Modal Parameters on Response-Only Data", *Journal of Sound and Vibration*, Vol. 259, No. 5, pp. 1163-1179, 2003.

34. Peeters, B., *System Identification and Damage Detection in Civil Engineering*, Ph.D. Thesis, Katholieke Universiteit Leuven, 2000.

35. Overschee P. V. and B. D. Moor, *Subspace Identification for Linear Systems*, Kluwer Academic Publishers, Dordrecht, 1996.

36. Asmussen, J. C. and R. Brincker, "A New Approach for Predicting the Variance of Random Decrement Functions", *The 16th International Modal Analysis Conference*, Santa Barbara, California, USA, 1998.

37. Ibrahim, S. R. and E. C. Mikulcik, "A New Method for the Direct Identification of Vibration Parameters from the Free Response", *Shock and Vibration Bulletin*, Vol. 47, No. 4, pp. 138-198, 1977.

38. Bendat, J. S. and A. G. Piersol, *Engineering Application of Correlation and Spectral Analysis*, Second Edition, John Wiley & Sons, Inc., New York, 1993.

39. Brinker, R., L. Zhang and P. Andersen, "Modal Identification of Output-Only System Using Frequency Domain Decomposition", *Smart Materials and Structures*, Vol. 10 No. 3, pp. 441–455, 2001.

40. Ewins, D. J., *Modal Testing: Theory and Practice*, Second Edition, Research Studies Press, Hertfordshire, 2000.

41. Shih, C. Y., Y. G. Tsuei, R. J. Allemang and D. L. Brown, "Complex Mode Indication Function and its Applications to Spatial Domain Parameter Estimation", *Mechanical Systems and Signal Processing*, Vol. 2, No. 4, pp. 367–377, 1988.

42. Google Maps, *The satellite image of the JRO*, 2012, https://maps.google.com/maps?q=Jamboree+Road,+Irvine,+CA,+United+States&hl=tr&ll=33.715284,-117.798876&spn=0.001682,0.002642&sll=33.683947,-117.794694&sspn=0.304537,0.676346&oq=irvine+jamboree&t=h&hnear=Jamboree+Rd,+Irvine,+California&z=19, accessed at July 2012.

43. Transportation Corridor Agencies, *JRO Technical Drawings*, California Department of Transportation, C22467, 1997.

44. Google Street View, *Photo of the JRO*, 2011, http://maps.google.co.uk/maps?q=Jamboree+Road,+Irvine,+California,+United+States&hl=en&ll=33.716041,-117.798908&spn=0.003748,0.021136&sll=33.697066,-117.781162&sspn=0.076123,0.169086&oq=california+irvine+jamb&t=h&hnear=Jamboree+Rd,+Irvine,+California,+United+States&z=16&layer=c&cbll=33.715755,-117.798899&panoid=X0BYfpIqE8v4kS64twxzVw&cbp=12,128.56,,0,-2.28, accessed at July 2012.

45. Gomez, H. C., *System Identification of Highway Bridges Using Long-Term Vibration Monitoring Data*, Ph.D. Thesis, University of California, Irvine, 2011.

46. Federal Highway Administration, *Seismic Bridge Design Applications*, U.S. Department of Transportation, *FHWA-SA-97- 017*, 1996.

47. Pan, T. C. and J. Li, "Dynamic Vehicle Element Method for Transient Response of Coupled Vehicle-Structure Systems", *Journal of Structural Engineering*, Vol. 128, No. 2, pp. 214–223, 2002.

48. Kwon, S. D., C. Y. Kim and S. P. Chang, "Change of Modal Parameters of Bridge Due to Vehicle Pass", *The 2005 IMAC-XXIII: Conference & Exposition on Structural Dynamics*, Orlando, Florida, USA, 2005.

49. Green, M. F. and D. Cebon, "Dynamic Response of Highway Bridges to Heavy Vehicle Loads: Theory and Experimental Validation", *Journal of Sound and Vibration*, Vol. 170, No. 1, pp. 51-78, 1994.

50. Yang Y. B., B. H. Lin, "Vehicle–Bridge Interaction Analysis by Dynamic Condensation Method", *Journal of Structural Engineering*, Vol. 121, No. 11, pp. 1636–1643, 1995.

51. Fryba, L., *Vibration of Solids and Structures under Moving Loads*, Noordholf International Publishing, Groningen, 1972.